Palmitoylation is required for the production of a soluble multimeric Hedgehog protein complex and long-range signaling in vertebrates

Miao-Hsueh Chen,[1] Ya-Jun Li,[1] Takatoshi Kawakami, Shan-Mei Xu, and Pao-Tien Chuang[2]

Cardiovascular Research Institute, University of California, San Francisco, California 94143, USA

Hedgehog (Hh) signaling plays a major role in multiple aspects of embryonic development. A key issue in Hh signaling is to elucidate the molecular mechanism by which a Hh protein morphogen gradient is formed despite its membrane association. In this study, we used a combination of genetic, cellular, and biochemical approaches to address the role of lipid modifications in long-range vertebrate Hh signaling. Our molecular analysis of knockout mice deficient in *Skn*, the murine homolog of the *Drosophila ski* gene, which catalyzes Hh palmitoylation, and gene-targeted mice producing a nonpalmitoylated form of Shh indicates that Hh palmitoylation is essential for its activity as well as the generation of a protein gradient in the developing embryos. Furthermore, our biochemical data show that Hh lipid modifications are required for producing a soluble multimeric protein complex, which constitutes the major active component for Hh signaling. These results suggest that soluble Hh multimeric complex travels in the morphogenetic field to activate Hh signaling in distant Hh-responsive cells.

[*Keywords*: Cholesterol; palmitoylation; Hedgehog; lipid modification; signaling; multimerization]

Supplemental material is available at http://www.genesdev.org.

Received January 13, 2004; revised version accepted February 19, 2004.

Hedgehog (Hh) signaling plays a key role in inductive interactions in various tissues during vertebrate development, and deregulation of the pathway in human is associated with various congenital anomalies and tumors (Ingham and McMahon 2001; McMahon et al. 2003). Insights emerging from classical embryology combined with molecular characterization of Hh signaling have provided a paradigm for understanding the fundamental principles of vertebrate development. In many places, while *Sonic hedgehog* (*Shh*) mRNA is localized to signaling centers (Echelard et al. 1993; Riddle et al. 1993), a Shh protein gradient, emanating from the signaling centers, is generated (Gritli-Linde et al. 2001), consistent with its role in long-range signaling in a dose-dependent manner. For example, *Shh* expression in the notochord and floor plate patterns the ventral neural tube as well as the sclerotome of the somites (Echelard et al. 1993; Fan and Tessier-Lavigne 1994; Marti et al. 1995; Roelink et al. 1995; Chiang et al. 1996). Similarly, *Shh* expression in the zone of polarizing activity (ZPA) specifies digit identity along the anteroposterior axis of the developing limbs (Riddle et al. 1993; Chiang et al. 1996; Yang et al. 1997; Lewis et al. 2001). Elucidation of the molecular mechanism by which a Hh protein gradient is generated is key to understanding how a single signal elicits multiple responses in a temporally and spatially specific manner. In this regard, a central question in Hh signaling is to understand how membrane-anchored Hh ligand, due to lipid modifications, travels in the morphogenetic field to generate a protein gradient. Likely, novel cellular mechanisms are used in this process.

Among the many striking features of Hh signaling is the unusual dual lipid modification (Porter et al. 1996; Pepinsky et al. 1998), which appears to be critical for proper Hh signaling. A Hh precursor molecule undergoes autoproteolytic cleavage to generate an N-terminal frag-

[1]These authors contributed equally to this work.
[2]Corresponding author.
E-MAIL chuang@cvrimail.ucsf.edu; FAX (415) 476-2283.
Article and publication are at http://www.genesdev.org/cgi/doi/10.1101/gad.1185804.

ment (Hh-N), the mature form of which (denoted as Hh-Np; p indicates processed) becomes membrane-anchored presumably due to the addition of a palmitoyl moiety to its N terminus (Pepinsky et al. 1998) and a cholesterol group to the C terminus (Porter et al. 1996). Although the cleavage event is a prerequisite for cholesterylation, in vitro studies using purified proteins also inferred that cholesterol modification may precede palmitoylation during Hh protein maturation (Pepinsky et al. 1998). Lipid modification could potentially affect the in vivo biological activities of Hh protein in at least two ways. Overexpression studies suggest that lipid-modified Hh proteins have higher activities than nonlipid-modified Hh proteins (Kohtz et al. 2001; Lee et al. 2001), although the molecular mechanism underlying the increased activity is not known. Furthermore, membrane association of the Hh protein could lead to altered protein distribution.

To directly address the role played by cholesterol modification in Hh signaling during vertebrate development, mice were generated by gene targeting in which only the N-terminal fragment (Shh-N) lacking cholesterol was produced (Lewis et al. 2001). These animals exhibited multiple phenotypes due to defective Hh signaling. Remarkably, in the limbs, digits with anterior identities did not form due to reduced long-range Hh signaling, whereas short-range Hh signaling to induce posterior digits appeared to be intact. This unexpected finding highlighted the importance of cholesterol modification in long-range Hh signaling, which stands in contrast to the traditional view that a membrane-anchored protein is unlikely to be transported in the morphogenetic field. The biochemical mechanism by which lipid-modified Hh protein is transported is not known. It is also not clear to what extent Shh-N protein produced in the *Shh-N* animals is palmitoylated; hence the relative phenotypic contributions due to lack of cholesterol or palmitate cannot be assessed.

Less has been revealed with respect to the role of Hh protein palmitoylation during vertebrate development. Although overexpression studies in mice suggested that Hh protein lacking palmitoylation is less active in some tissues (Kohtz et al. 2001; Lee et al. 2001), the in vivo function of Hh palmitoylation in vertebrates has not been fully investigated. Instead, significant insights into the role of palmitoylation in Hh signaling came from the identification of the *Drosophila sightless/skinny hedgehog/central missing/rasp* gene (denoted as *ski* in this study; Amanai and Jiang 2001; Chamoun et al. 2001; Lee and Treisman 2001; Micchelli et al. 2002), which was shown to be involved in Hh palmitoylation. Fly mutants deficient in both maternal and zygotic *ski* function die during embryogenesis with aberrant patterning resembling that observed in other mutants defective in Hh signaling. *Drosophila ski* encodes a putative acyltransferase, presumably catalyzing the transfer of a palmitoyl moiety to the Hh N terminus. Mosaic analysis indicates that *ski* is required in Hh-producing cells and thus likely plays an essential role in a maturation event (palmitoylation) critical for activity of the Hh signal (Amanai and Jiang 2001; Chamoun et al. 2001; Lee and Treisman 2001; Micchelli et al. 2002).

Although it is not known how a Hh protein gradient is generated, studies using cultured cells as well as limb buds suggested that long-range Shh signaling could potentially involve the production of a soluble multimeric Shh-Np complex (Zeng et al. 2001). The Shh-Np molecule is thought to self-associate and form a globular multimeric protein complex with its hydrophobic lipid-modified N and C termini buried inside (Zeng et al. 2001; Ho and Scott 2002). Whether additional proteins other than Shh are present in the protein complex is not clear (the complex will simply be referred to as Shh multimeric complex in this study). It was also found that conditioned media containing soluble Shh-Np, including multimeric and monomeric forms, is at least 15 times more potent than that containing soluble Shh-N, which lacks cholesterol modification (Zeng et al. 2001). The roles that cholesterol and palmitate modification play in the formation of multimeric Shh-Np is not known. In addition, whether multimeric Shh-Np exists and forms a protein gradient in the animal has never been directly shown. Diffusion is unlikely to be the sole mechanism by which soluble Shh-Np is transported because studies in *Drosophila* have identified genes essential for transporting Hh protein once they are released from Hh-producing cells (Bellaiche et al. 1998; The et al. 1999; Han et al. 2004; Takei et al. 2004).

Because many aspects of Hh signaling are highly conserved from fly to mammals (Ingham and McMahon 2001), it is surprising that the roles of lipid modifications in *Drosophila* versus vertebrate Hh signaling do not seem to be identical. First, cholesterol was shown to be required for long-range Hh signaling in mammals through the studies of a *Shh-N* allele (Lewis et al. 2001). In contrast, overexpression of *Drosophila* Hh-N lacking cholesterol actually produced a wider range of signaling than that of wild-type Hh (Burke et al. 1999). Furthermore, the effects of palmitoylation on Hh protein activity appear to be different between *Drosophila* and vertebrate Hh protein. Overexpression of *Drosophila* Hh lacking palmitoylation, Hh^{C85S}, exerted dominant-negative effects on Hh signaling and did not activate the Hh pathway (Lee et al. 2001). In comparison, in vertebrates, Shh lacking palmitoylation, when overexpressed in the forebrain and the limb, leads to ectopic activity (Kohtz et al. 2001; Lee et al. 2001). Whether *Drosophila* Hh protein can form a multimeric complex, like vertebrate Hh protein, has not been reported. These results could potentially reflect a difference in the biochemical properties of Hh proteins and/or a differential tissue response to Hh signaling in diverse species.

To establish the role of Hh palmitoylation during vertebrate development, here we report the molecular analysis of knockout mice deficient in the murine homolog of the *Drosophila ski* gene and gene-targeted mice producing a nonpalmitoylated form of Shh. We also present biochemical studies that provide significant insights into the role of lipid modifications in generating a soluble form of Hh multimeric protein complex

and suggest a model of how a Hh protein gradient is formed.

Results

Vertebrate Hedgehog proteins with differential lipid modification exhibit different activities in vivo

An important issue in understanding the roles of lipid modification in vertebrate Hh signaling is whether various lipid-modified forms of Hh protein possess different biological activities in vivo. We addressed this issue by using a transgenic approach in mice in order to achieve better control of expression levels. cDNAs encoding different forms of murine Hh protein—including (1) wild-type Shh; (2) Shh^{C25S}, which lacks palmitoylation; and (3) Shh-N^{C25S}, which undergoes neither palmitoylation nor cholesterylation—were expressed throughout the mesenchyme of developing mouse limb buds under the control of the *Prx1* promoter/enhancer (Logan et al. 2002). Purified insert DNA at the concentration of 0.5 ng/μL from all three constructs was injected into the pronuclei of fertilized eggs. Embryos were collected at 18.5 days postcoitum (dpc), and skeletal preparations were performed to assess the digit pattern. Transgenic mice expressing wild-type *Shh* displayed digit duplication in both forelimbs (Fig. 1B) and hindlimbs (Fig. 1F). Slight variation exists from animal to animal, with total number of digits ranging from 14 to 16 in the forelimbs and 12 to 15 in the hindlimbs (Table 1). In addition, duplicated digits appear to lose their identity, similar to what was observed in *Gli3* mutant limbs, in which loss of Gli3 leads to active Hh signaling across the limb field (Litingtung et al. 2002; te Welscher et al. 2002). Transgenic mice expressing Shh^{C25S} also exhibited digit duplication in both forelimbs (Fig. 1C) and hindlimbs (Fig. 1G), but digit duplication beyond seven per limb was never observed (Table 1). In addition, digit identity is maintained in Shh^{C25S} transgenics, indicating a lower level of Hh signaling. Finally, digit duplication in transgenic animals expressing Shh-N^{C25S} (Fig. 1D,H) appears to be even less pronounced than those expressing Shh or Shh^{C25S} (Table 1). Taken together, these results suggest that vertebrate Hh protein without palmitoyl modification has reduced activity in inducing Hh responses, and Hh protein lacking any lipid modification possesses even lower levels of residual activity.

Mouse embryos deficient in the Skinny hedgehog *(*Skn*) gene exhibit defects in the developing neural tube and limb due to defective long-range Shh signaling as well as in the skeleton due to defective Indian hedgehog (Ihh) signaling*

To further understand the role of palmitoylation in vertebrate Hh signaling in vivo, we investigated the functions of the vertebrate *Skinny hedgehog* (*Skn*) gene, which encodes a putative acyltransferase (see Materials and Methods). *Skn* mRNA could be detected on Northern blots as early as 7.0 dpc (data not shown). *Skn* is broadly expressed during mouse embryonic development (Fig. 2N–P) with higher levels of expression in the anterior ectoderm, pharyngeal arches, and the distal part of the limb at 10.5 dpc. To define the roles of *Skn* in Hh signaling during vertebrate development, we generated two null alleles of *Skn* using gene targeting in mice (Supplementary Figs. 1, 2). *Skn* is located on mouse chromosome 1, and the genomic locus consists of 11 relatively small exons. We targeted the second and ninth exons, respectively, to generate null alleles of *Skn* because the second exon contains the translational start and the ninth exon contains predicted active sites for an acyltransferase (Hofmann 2000). As described below, both alleles generate identical phenotypes, which likely represent the null phenotype; thus we will refer to them simply as the *Skn* allele in this study.

Homozygous *Skn* embryos can be clearly identified at 10.5 dpc by their smaller size and holoprosencephaly (Fig. 2B), a hallmark of defective *Shh* signaling, although these defects are less pronounced than those in *Shh* mutants (Fig. 2D; Chiang et al. 1996). As development proceeds, at 13.5 dpc obvious shortening of the limbs was observed, and at birth the mutant animals exhibited severe short-limb dwarfism (Fig. 2B′), remarkably similar to that of *Ihh* mutants (Fig. 2D′; St-Jacques et al. 1999). Homozygous *Skn* mutants developed to term but died soon after birth. Consistent with the characteristic phenotypes indicative of defective Hh signaling, expression of Hh target genes, such as *Ptc1* (Fig. 2I,I″; Goodrich et al. 1996) and *Hip1* (Fig. 2I′; Chuang and McMahon 1999), is greatly reduced in *Skn* mutants, whereas *Shh* (Fig. 2F,F′) and *Ihh* (Fig. 2F″) expression levels cannot be distinguished from those of their wild-type littermates (Fig. 2E,E′,E″). These results indicate that *Skn* is required for wild-type levels of both *Shh* and *Ihh* signaling during mammalian development.

We focused our analysis on the developing neural tube and limb, where Hh signaling has been extensively studied and both short- and long-range signaling are used in patterning these structures (McMahon et al. 2003). In the ventral spinal cord, a combinatorial code of homeodomain transcription factors defines and specifies five progenitor cell types (Vp0, Vp1, Vp2, pMN, and Vp3; Fig. 3; Briscoe and Ericson 1999, 2001). These progenitors subsequently generate five distinct neuronal types (v0, v1, v2, MN, and v3). Previous studies suggest that expression of *Shh* in the notochord acts short-range to induce the floor plate (Le Douarin and Halpern 2000; Placzek et al. 2000). Subsequently, Hh signaling from the notochord and floor plate acts long-range to regulate expression of homeodomain transcription factors essential for proper generation of ventral motor neurons and interneurons (Briscoe and Ericson 2001). *Shh* mutant embryos generate v0, v1, and occasionally v2 interneuron precursors at forelimb levels (Pierani et al. 1999; Litingtung and Chiang 2000), indicating that *Shh* signaling is required for the generation of the Vp2, pMN, and Vp3 progenitor pools. Interestingly, *Smoothened* (*Smo*), which is essential for all Hh signaling, is required for the specification

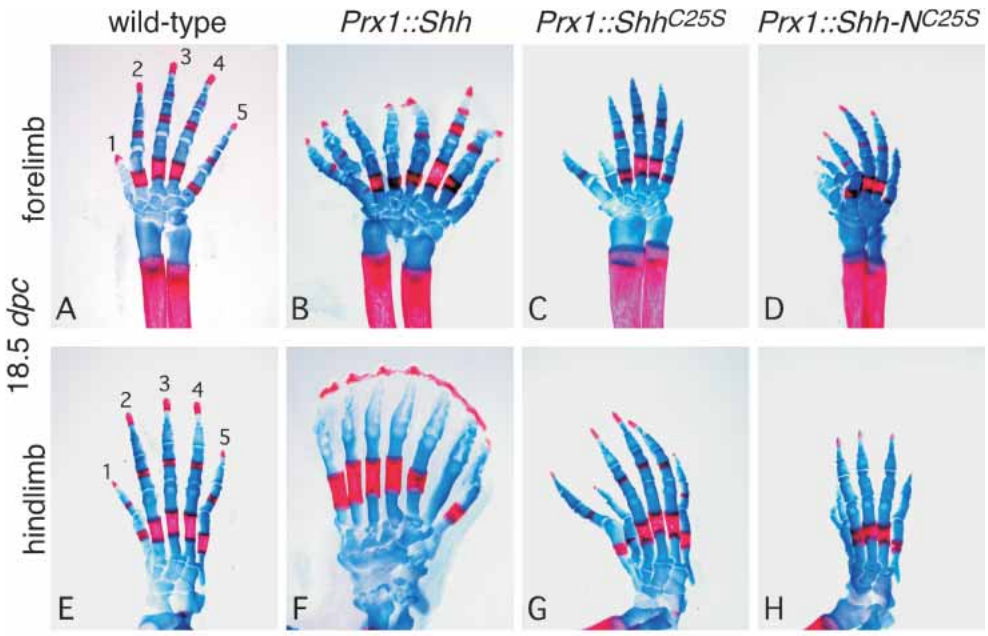

Table 1

		Forelimb (0.5 ng/μl)							Hindlimb (0.5 ng/μl)						
Total number of digits (both limbs)		10	11	12	13	14	15	16	10	11	12	13	14	15	16
Number of pronuclear injected embryos	Non-transgenics (n=135)	135							135						
	Prx1::Shh (n=10)					3	6	1			4	2	3	1	
	Prx1::Shh^{C25S} (n=7)		3	1	3					2	2	2			
	Prx1::Shh-N^{C25S} (n=6)	3	2			1					6				

Figure 1. The activity of Hedgehog proteins with differential lipid modification in transgenic animals. Fore- and hindlimb skeleton (stained with Alcian blue [cartilage] and Alizarin red [calcified tissue]) of 18.5-dpc wild-type (*A*,*E*) and transgenic mice expressing *Shh* (*B*,*F*), *Shh*^{C25S} (*C*,*G*), and *Shh-N*^{C25S} (*D*,*H*) in the limb mesenchyme under the *Prx1* promoter/enhancer. Views are all dorsal. The axis for orientation of the specimens is posterior on the right, anterior on the left, proximal downward, and distal upward. Table 1 summarizes the distributions of digit duplication in both fore- and hindlimbs of nontransgenic and transgenic animals expressing various forms of Shh proteins in the limb. Digits from both left and right limbs were counted, with 10 digits in nontransgenic wild-type mice. Compared with the hindlimbs, the forelimbs are more sensitive in their response to varying activities of Shh. Although the integration site of the transgene could potentially affect its expression levels, a general trend of decreasing activity from Shh to Shh-N^{C25S} could be obtained by examining multiple transgenic animals. The DNAs were quantified and adjusted to 0.5 ng/μL for pronuclear injection.

of all ventral neural progenitor populations, suggesting that *Ihh* patterns some ventral cell types in *Shh* mutants (Wijgerde et al. 2002). Hh signaling from the notochord and floor plate is also required for expanding sclerotomal fates (Fan et al. 1995; Chiang et al. 1996). In *Skn* mutants, *Shh* is expressed in the notochord, but *Shh* (Fig. 2F′) and *HNF3*β (Fig. 2R; Ang et al. 1993; Sasaki and Hogan 1993; data not shown) are not detected in the ventral midline of the neural tube except at the more rostral and caudal regions where residual *Shh* and *HNF3*β expression in the ventral midline could be detected (Fig. 2R, arrows). However, no morphologically distinct floor plate could be identified at all axial levels.

These results indicate that *Skn* is required for short-range Shh signaling in the axial midline. To examine whether dorsoventral patterning of the neural tube, which requires long-range *Shh* signaling in a dose-dependent manner, is affected, we probed the expression of molecular markers that define different progenitor domains as well as markers for the differentiated interneurons and motorneurons. For instance, the expression domain of *Dbx1*, the ventral boundary of which marks the progenitor domain of v0 interneurons (Fig. 3A), is shifted toward the ventral midline in *Skn* mutants (Fig. 3B). *Nkx6.1*, which is expressed in regions encompassing the progenitor domains of v2 interneurons, motor neurons,

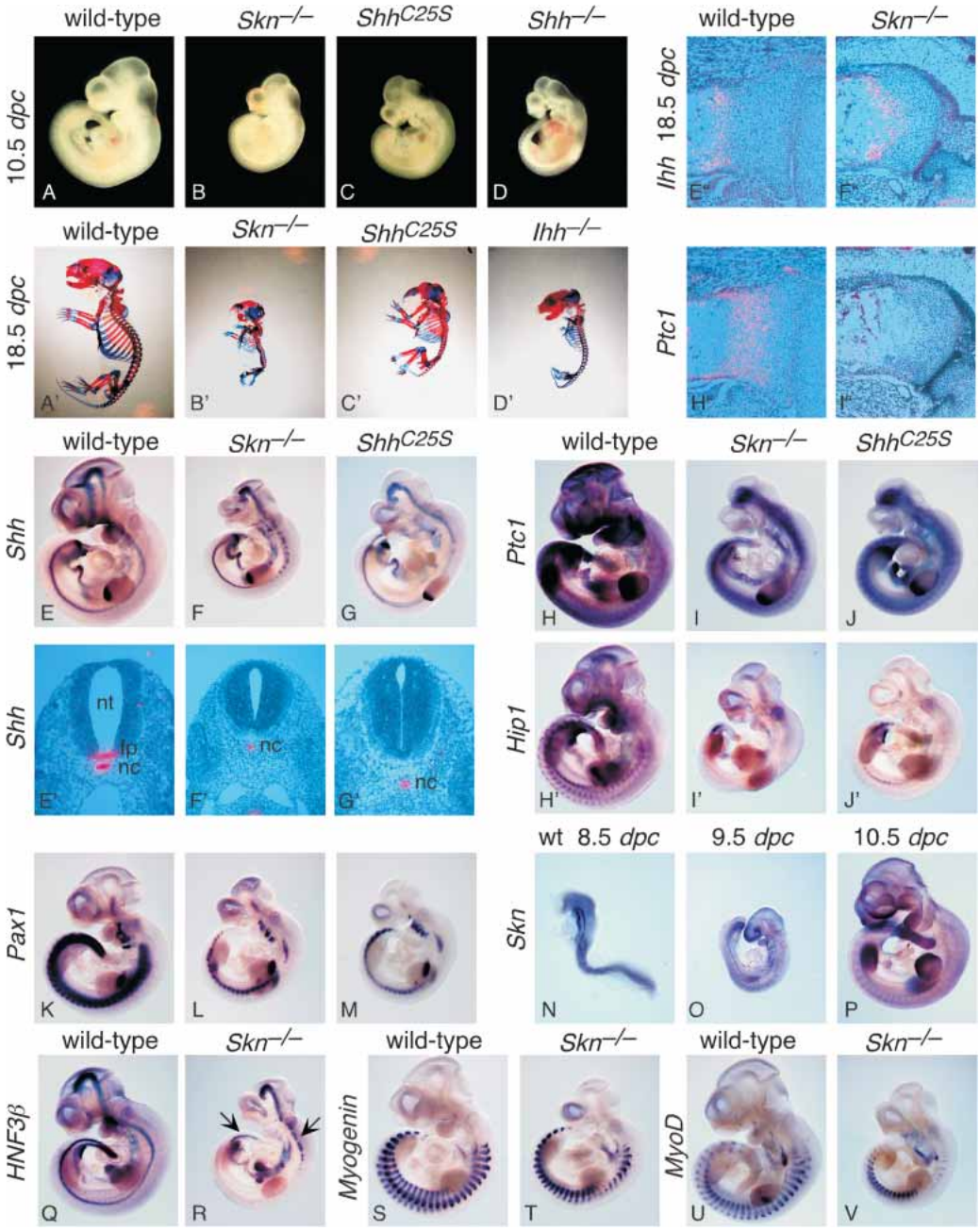

Figure 2. *Skn* and Shh^{C25S} mutants exhibit multiple defects due to reduced Hh signaling. (*A–D*) External morphology of wild-type, $Skn^{-/-}$, Shh^{C25S}, and $Shh^{-/-}$ embryos at 10.5 dpc. All views are lateral. (*A′–D′*) Skeleton of wild-type, $Skn^{-/-}$, Shh^{C25S}, and $Ihh^{-/-}$ 18.5-dpc embryos stained with Alcian blue and Alizarin red. All views are lateral. Embryos in *A–D* and *A′–D′* were photographed at the same magnification, respectively. (*E–V*,*H′–J′*) Whole-mount in situ hybridization, using digoxigenin-labeled riboprobes on wild-type, $Skn^{-/-}$, and Shh^{C25S} embryos at 10.5 dpc with the exceptions of *N* (8.5 dpc) and *O* (9.5 dpc). All views are lateral. Expression of *Hip1* is known to be completely dependent on Hh signaling (Chuang and McMahon 1999), whereas *Ptc1* expression is initially Hh independent but is strongly up-regulated upon Hh signal transduction (Goodrich et al. 1996). Arrows in *R* point to residual *HNF*3β expression in the more rostral and caudal part of the ventral midline of the neural tube. Expression of Myogenin and MyoD (Tajbakhsh et al. 1997) in $Skn^{-/-}$ mutants cannot be readily distinguished from that in wild-type embryos. Embryos in *E–G*; *H–J*; *H′–J′*; *K–M*; *Q* and *R*; *S* and *T*; and *U* and *V* were photographed at the same magnification, respectively. (*E′–G′*) Isotopic in situ hybridization using ^{33}P-UTP-labeled riboprobes (pink) on paraffin sections of wild-type, $Skn^{-/-}$, and Shh^{C25S} 10.5-dpc embryos at the forelimb/heart level. (*E″*,*F″*,*H″*,*I″*) Isotopic in situ hybridization using ^{33}P-UTP-labeled riboprobes (pink) on paraffin sections of proximal tibia of wild-type and femur of $Skn^{-/-}$ 18.5-dpc embryos. Expression of *Ptc1* in the chondrocytes is regulated by *Ihh* and not *Shh* (St-Jacques et al. 1999). (Nt) Neural tube; (fp) floor plate; (nc) notochord.

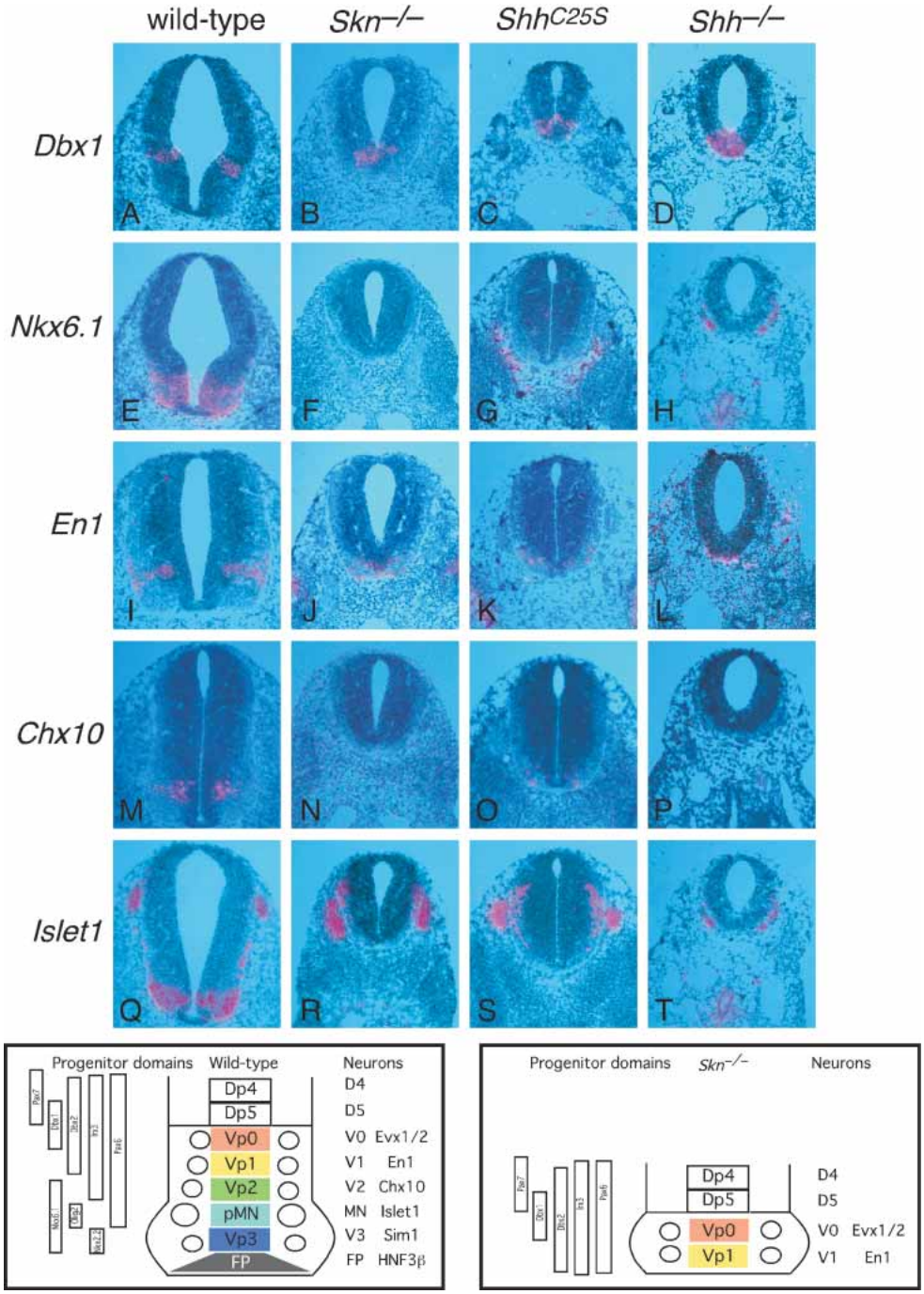

Figure 3. *Skn* and *Shh*^{C25S} mutants exhibit defective short- and long-range signaling in the neural tube. (*A–T*) Isotopic in situ hybridization using ^{33}P-UTP-labeled riboprobes (pink) on paraffin sections of wild-type, *Skn*$^{-/-}$, *Shh*^{C25S}, and *Shh*$^{-/-}$ 10.5-dpc embryos at the forelimb/heart level. The *bottom left* panel shows a schematic diagram of the expression domains of transcription factors, a combination of which define five progenitor cell types (Vp0, Vp1, Vp2, pMN, and Vp3) in wild-type embryos. As a result, five distinct neuronal types (v0, v1, v2, MN, and v3) are generated, which could be identified by neuronal-specific markers. In *Skn* mutants (*bottom right* panel) as well as in *Shh*^{C25S} mutants, reduced Hh signaling leads to loss of floor plate, v3, MN, and most v2 with concomitant changes in the progenitor domains. This phenotype is similar to that in *Shh*$^{-/-}$ mutants perhaps with the exception of v2, a greater proportion of which is present in *Skn* and *Shh*^{C25S} mutants. Similarly, the *Shh*^{C25S} phenotype is slightly less severe than that in *Skn* mutants judged by residual v2. Expression of *Islet1* in *R–T* represents neural crest-derived ganglia.

and v3 interneurons in wild-type embryos (Fig. 3E), is barely detectable in *Skn* mutants (Fig. 3F). Meanwhile, the expression domains of other progenitor markers are either shifted toward the ventral midline (e.g., *Dbx2*,

Pax6, and *Pax7*; data not shown) or are absent (e.g., *Nkx2.2*; data not shown). These results suggest that most v2 interneurons, motor neurons, and v3 interneurons are not present in *Skn* mutants. Consistent with this conclusion, expression of *Chx10* (a marker of v2 interneurons; Fig. 3N), *Islet1* (a marker for motor neurons; Fig. 3R), and *Sim1* (a marker for v3 interneurons; data not shown) is missing in *Skn* mutants, whereas expression of *Evx1/2* (a marker for v0 interneurons; data not shown) and *En1* (a marker for v1 interneurons; Fig. 3J) is shifted toward the ventral midline in *Skn* mutants. These results indicate that *Skn* is required for long-range Shh signaling in the neural tube, and the phenotype in the ventral tube is quite similar to that in *Shh* mutants (Fig. 3D,H,L,P,T; data not shown). Expression of the sclerotomal marker *Pax1* (Deutsch et al. 1988) is markedly reduced in *Skn* mutants (Fig. 2L), indicating that *Skn* is also required for long-range signaling from the notochord and floor plate to expand sclerotomal fates.

We next investigated the role of *Skn* in limb patterning. Here it appears that both *Shh* and *Ihh* signaling are affected in *Skn* mutants, albeit to different degrees. The *Skn* mutant skeleton (Figs. 2B′, 4C,C′) is remarkably similar to that in *Ihh* mutants (Fig. 2D′). The *Skn* mutant limbs displayed severe dwarfism, with markedly reduced chondrocyte proliferation (Fig. 4D,D′) reminiscent of *Ihh* mutants (St-Jacques et al. 1999). In contrast, the digit defect in *Skn* mutants (Fig. 4C,C′) due to reduced *Shh* signaling from the ZPA is not as pronounced as that in *Shh* mutants (Fig. 4G,G′; Chiang et al. 1996; Kraus et al. 2001). It has been shown that the anterior digit 1 still forms in the complete absence of *Shh* (Kraus et al. 2001), indicating that specification of digits 2 through 5 requires long-range Shh signaling. In gene-targeted mice expressing the N-terminal fragment of Shh (Shh-N) lacking cholesterol modification, digits 1, 4, and 5 are specified but digits 2 and 3 are missing (Lewis et al. 2001). Interestingly, when the *Ptc1* dosage is reduced in the limbs of Shh-N embryos, five digits (5, 4, 2, 1, and 1) are generated (Lewis et al. 2001). These results were interpreted as a requirement of cholesterol modification for long-range signaling in the limb. In addition, reducing *Ptc1* levels leads to an anterior enlargement of the Shh-N signaling domain, presumably due to decreased sequestration of Shh-N by Ptc1 (Lewis et al. 2001). Because Shh-N may be less efficiently palmitoylated (Pepinsky et al. 1998), the phenotypes in *Shh-N* mice could be attributed to a combined effect of lacking both cholesterol and, to some extent, palmitoylation. The *Skn* mutants provide an opportunity to directly test the role of palmi-

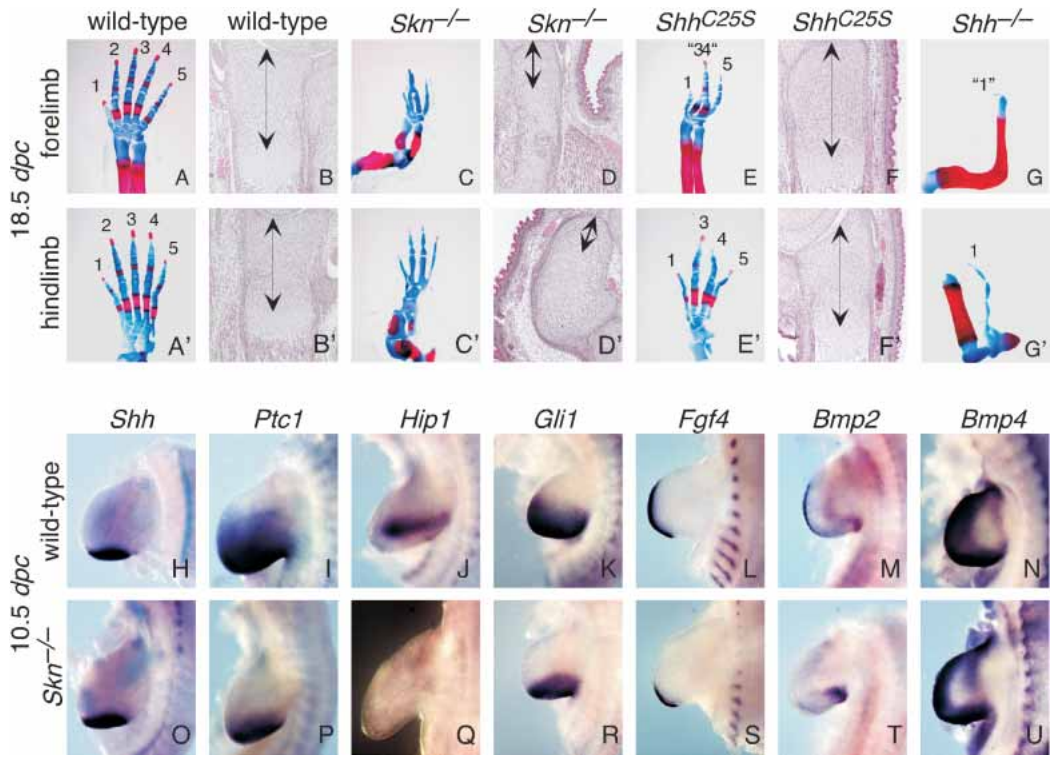

Figure 4. *Skn* and Shh^{C25S} mutants have defective long-range Hedgehog signaling in the limb. (*A*,*A*′,*C*,*C*′,*E*,*E*′,*G*,*G*′) Fore- and hindlimb skeletons of wild-type, $Skn^{-/-}$, Shh^{C25S}, and $Shh^{-/-}$ 18.5-dpc embryos stained with Alcian blue and Alizarin red. All views are dorsal. The axis for orientation of the specimens is posterior on the right, anterior on the left, proximal downward, and distal upward. (*B*,*B*′,*D*,*D*′,*F*,*F*′) Hematoxylin-and-eosin-stained sections through the distal ulnar and tibia of wild-type, $Skn^{-/-}$, Shh^{C25S}, and $Shh^{-/-}$ 18.5-dpc embryos. Arrows indicate immature chondrocytes. (*H–U*) Whole-mount in situ hybridization, using digoxigenin-labeled riboprobes on wild-type and $Skn^{-/-}$ limbs at 10.5 dpc. *Bmp4* expression in $Skn^{-/-}$ limbs cannot be distinguished from that in wild-type limbs (Jones et al. 1991).

toylation in *Shh* signaling in the limb and also allow us to assess the relative contributions of cholesterol and palmitate modifications in Hh signaling. In *Skn* mutants, like *Shh-N* mutants (Lewis et al. 2001), no proximal-distal truncation of limb elements, which occurs in the absence of *Shh* (Chiang et al. 1996), was observed. However, only four digits (most likely digits 1 and 3–5) form (Fig. 4C,C′). In most *Skn* mutants, fusion between digits 3 and 4 in the forelimb (Fig. 4C) was also observed. These results suggest that in *Skn* mutants, *Shh* still possesses a "sufficient" level of posterior signaling activity that can specify the most posterior digit 5. However, long-range signaling to the anterior regions to specify digit 2 (and possibly digit 3) is affected. A molecular analysis of markers indicates that expression of Hh-responsive genes, such as *Ptc1* (Fig. 4P), *Hip1* (Fig. 4Q), and *Gli1* (Fig. 4R), is greatly reduced in *Skn* limb buds, whereas *Shh* expression (Fig. 4O) is unchanged. *Fgf4* expression in the apical ectodermal ridge (AER; Niswander and Martin 1992; Suzuki et al. 1992) is more posteriorly restricted in *Skn* mutants (Fig. 4S) due to anterior truncation of Hh signaling.

Mouse embryos expressing Shh protein lacking palmitoylation (Shh^{C25S}) exhibit similar defects to those in Skn-deficient embryos due to defective Shh signaling

If the phenotypes observed in *Skn* mutants are solely due to lack of palmitoylation of the Hh proteins, one would predict that mice expressing only the nonpalmitoylated form of Hh would exhibit similar phenotypes to those in *Skn* mutants. In contrast, if Skn has targets other than Hh proteins, *Skn* mutants may exhibit a spectrum of phenotypes not present in mutants carrying the nonpalmitoylated form of Hh. To distinguish between these possibilities, we used gene targeting in mice to introduce a single base change into the *Shh* genomic locus (the resulting allele is designed Shh^{C25S}; Supplementary Fig. 3). This generated a Cys-to-Ser change at amino acid position 25 and abolished palmitoylation of Shh protein.

Homozygous Shh^{C25S} embryos can be clearly identified at 10.5 dpc by their smaller size and holoprosencephaly (Fig. 2C), and their appearance is remarkably similar to that of *Skn* mutants (Fig. 2B). As development proceeds, Shh^{C25S} mutants continue to exhibit phenotypes resembling those of *Skn* mutants (Fig. 2B′), with the exception that no obvious skeletal defects were observed in Shh^{C25S} mutants (Fig. 2C′). Similar to *Skn* mutants, homozygous Shh^{C25S} mutants developed to term and died soon after birth.

We performed a detailed phenotypic and molecular analysis on the neural tube and limb of Shh^{C25S} mutants, essentially identical to that described above for *Skn* mutants. In the neural tube of Shh^{C25S} mutants, most v2 interneurons, motor neurons, and v3 interneurons are missing (Fig. 3C,G,K,O,S; data not shown), similar to that in *Skn* mutants. A direct comparison between *Skn* and Shh^{C25S} mutants indicates that more v2 neurons are present in Shh^{C25S}, suggesting that *Skn* neural tube defects are slightly more severe than those in Shh^{C25S} mice and likely due to defective Ihh signaling in *Skn* mice. In the limb, only four digits (digits 1 and 3 through 5) form in Shh^{C25S} mutants and fusion between digits 3 and 4 was also observed in most mutant forelimbs (Fig. 4E,E′), similarly to those in *Skn* mice. Animals expressing one copy of Shh^{C25S} and one copy of a *Shh* null allele (Shh^{n}) do not exhibit more severe phenotypes than those in homozygous Shh^{C25S} mutants (data not shown). Interestingly, in contrast to the *Shh-N* allele (Lewis et al. 2001), reducing the dosage of *Ptc1* in Shh^{C25S} or Shh^{C25S}/Shh^{n} mutants has no apparent effects on digit patterning (data not shown). Taken together, these results indicate that *Skn* and Shh^{C25S} share similar phenotypes due to defective Shh signaling and Hh proteins are likely the major targets of Skn during embryonic development.

Hedgehog protein is properly processed but its distribution is restricted mainly to the sites of synthesis in Skn and Shh^{C25S} mutants

Because the *Shh* mRNA expression level appears to be normal in both *Skn* (Fig. 2F) and Shh^{C25S} (Fig. 2G) mutants, we asked whether processing of Shh to generate a cholesterol-modified N-terminal fragment of Shh also occurs normally in *Skn* and Shh^{C25S} mutants. Lysates from wild-type, *Skn*, and Shh^{C25S} embryos collected at 10.5 dpc were separated by SDS-PAGE for Western blotting. Shh antibodies recognized the unprocessed as well as the processed form of Shh on Western blots, which ran at the same position as the cholesterol-modified N-terminal fragment in all lysates from wild-type, *Skn*, and Shh^{C25S} embryos (data not shown; Fig. 6B, below). This result suggests that Shh processing and cholesterol modification occur normally in *Skn* or Shh^{C25S} mutants. In contrast, the addition of palmitate to Shh protein fails to occur in mutant cells derived from *Skn* embryos (Fig. 6B, left [below]). Skn is localized to the ER (revealed by anti-KDEL antibodies) in cultured cells (Fig. 5I,L), and Skn distribution largely overlaps with that of Shh (Fig. 5M,N,P). Taken together, these results indicate that Skn likely functions as an acyltransferase on Hh proteins in transit through the secretory pathway.

As a first step toward understanding the molecular mechanisms that underlie the defects in *Skn* and Shh^{C25S} mutants, we asked whether the distribution of Shh protein is affected in *Skn* or Shh^{C25S} mutants. In wild-type mouse embryos at 10.5 dpc, *Shh* mRNA expression at the axial midline is confined to the notochord and floor plate (Fig. 2E′; Echelard et al. 1993). In contrast, Shh protein can also be detected in Hh-responsive cells outside the notochord and floor plate (Fig. 5A; Gritli-Linde et al. 2001). Shh immunoreactivity is strong in the notochord and extends outward in a graded fashion (arrow in Fig. 5A), upward toward the ventral neural tube along the extracellular matrix (arrowhead in Fig. 5A) and downward toward the branchial pouch (Fig. 5A; Gritli-Linde et al. 2001; Kawakami et al. 2002). In *Skn* (Fig. 5B)

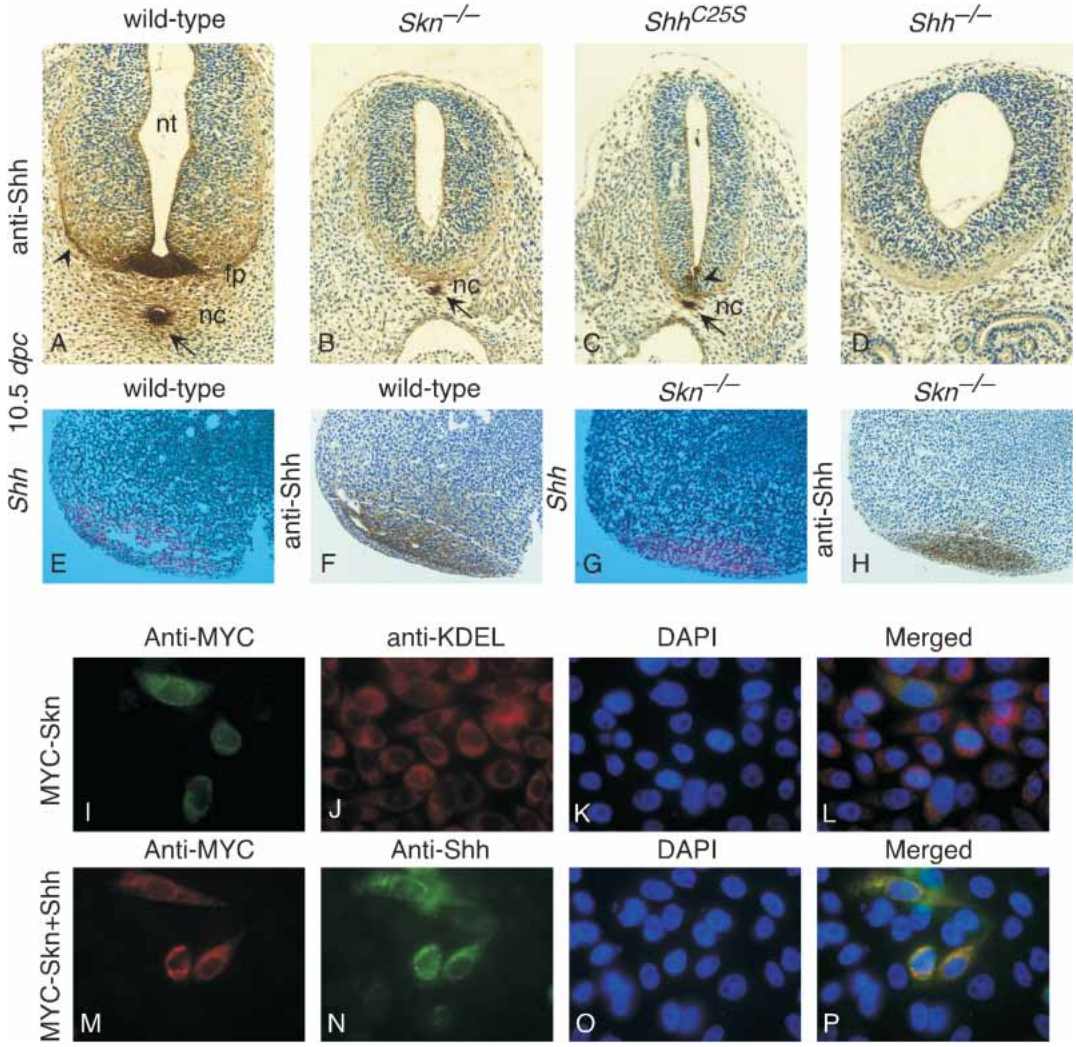

Figure 5. Shh protein is mainly restricted to its sites of synthesis in *Skn* and Shh^{C25S} mutants. (*A–D*) Cross-sections of wild-type, $Skn^{-/-}$, Shh^{C25S}, and $Shh^{-/-}$ embryos at 10.5 dpc at the forelimb/heart level stained with anti-Shh antibodies. In the wild-type section, Shh immunoreactivity (brown) is strong in the notochord and floor plate, and it extends out bidirectionally in a graded fashion (arrows and arrowheads). Similar patterns of Shh immunoreactivity extending from the notochord were observed on embryo sections where the floor plate has not yet been induced (Gritli-Linde et al. 2001), suggesting that Shh immunoreactivity in the neural tube is derived from both the notochord and floor plate. In sections of $Skn^{-/-}$ embryos, Shh immunoreactivity is mainly detected in the notochord (arrow), and no obvious extended staining is present. Similarly, Shh immunoreactivity is mainly detected in the notochord (arrow) of Shh^{C25S} embryos. In this section (*C*), residual Shh immunoreactivity could be detected in the ventral midline of the neural tube (arrowhead), but no obvious extension of staining to the neural tube was noted. This is due to a more posterior extension (to the forelimb level) of residual *Shh* mRNA expression in the ventral midline of the Shh^{C25S} neural tube at the more rostral levels (data not shown) than that in *Skn* mutants (Fig. 2R). Immunostaining was performed on multiple sections and on sections where Shh mRNA (Fig. 2E′–G′) or protein expression level in the notochord of $Skn^{-/-}$ and Shh^{C25S} mutants was comparable to that of wild-type; lack of spreading of Shh immunoreactivity was still observed. No Shh immunoreactivity is detected in the notochord or neural tube of $Shh^{-/-}$ embryos, although Shh immunoreactivity is detected in the gut of $Shh^{-/-}$ embryos, which represents cross reactivity to Ihh epitopes (data not shown). (*E,G*) Isotopic in situ hybridization using ^{33}P-UTP-labeled riboprobes (pink) on paraffin sections of wild-type and $Skn^{-/-}$ limbs at 10.5 dpc. *F* and *H* are adjacent sections to *E* and *G* and were stained with anti-Shh antibodies. The dotted pink lines in *F* and *H* represent the approximate domains of *Shh* mRNA expression as determined in *E* and *G*. Multiple limbs were sectioned, and in situ hybridization and immunostaining were performed on all sections from the limb. (*I–L*) CHO cells transiently transfected with an expression construct encoding a MYC-tagged Skn and stained with anti-MYC and anti-KDEL antibodies (ER marker). *L* is a merged image of *I–K*. (*M–P*) CHO cells cotransfected with expression constructs encoding MYC-SKN and Shh and stained with anti-MYC and anti-Shh antibodies. *P* is a merged image of *M–O*. Similar results were obtained by using HeLa cells (data not shown). (nt) Neural tube; (fp) floor plate; (nc) notochord.

or Shh^{C25S} (Fig. 5C) mutant embryos at this stage, Shh immunoreactivity is confined to the notochord (arrows in Fig. 5B,C), and immunoreactivity is barely detected in the neural tube. In the more rostral and caudal regions of

the neural tube where residual *Shh* mRNA expression can be detected, Shh immunoreactivity is confined to the ventral midline, corresponding to a subdomain of *Shh* mRNA expression, and immunoreactivity is barely detected in other parts of the neural tube (arrowhead in Fig. 5C; data not shown). Similarly, Shh protein distribution in the limb of *Skn* mutants (Fig. 5H) is mainly confined to the site of *Shh* mRNA synthesis in the ZPA (Fig. 5G), whereas Shh immunoreactivity could be detected in Hh-responsive cells outside the ZPA (Fig. 5F) in wild-type embryos at 10.75 dpc. These results are unlikely due to reduced Shh protein expression in *Skn* and *Shh^{C25S}* mutants because *Shh* mRNA expression (Figs. 2E,F, 4H,O) and protein expression by whole-mount immunostaining and Western blotting (data not shown) cannot be readily distinguished from that of wild-type embryos. Taken together, these results indicate that Shh lacking palmitoylation fails to generate a protein gradient in the morphogenetic field.

Hedgehog protein lacking palmitoylation can be targeted to lipid rafts but fails to generate a soluble multimeric protein complex

The observation that Hh protein lacking palmitoylation is not distributed to Hh-responsive cells at a distance from the Hh source prompted us to examine any changes in the biochemical properties of Hh protein in the absence of lipid modification, which could potentially underline the observed defects. Previous studies suggest that Hh proteins are associated with lipid raft microdomains in the membrane (Rietveld et al. 1999). In addition, palmitoylation of proteins is well known to play a key role in their sorting/targeting (Linder and Deschenes 2003). It is possible that Hh protein lacking palmitoylation fails to be anchored on the membrane, which subsequently affects its transport in the morphogenetic field. To test this hypothesis, we transfected HEK293 cells with four cDNA constructs encoding Shh, Shh^{C25S}, Shh-N, and Shh-N^{C25S}; isolated lipid raft fractions through sucrose gradient centrifugation; and examined the distribution of Hh proteins in different membrane fractions (Fig. 6A). A significant proportion of Shh was found in the lipid raft fractions as indicated by the presence of raft-resident proteins, Flotillin-1 (Fig. 6A), and caveolin (data not shown). Surprisingly, Shh^{C25S} and Shh-N can both be detected in lipid rafts, although the amount of Shh-N in lipid rafts is significantly lower (~50% by quantification) than that of either Shh or Shh^{C25S} (Fig. 6A; data not shown). In contrast, Shh-N^{C25S}, which lacks both lipid modifications, failed to reach the rafts (Fig. 6A). It is possible that a substantial proportion of Shh-N still undergoes palmitoylation, which allows membrane association. To test this, we transfected HEK293 cells with the above cDNA constructs in the presence of [^{3}H]-labeled palmitic acid. Indeed, labeled Shh-N was detected from cells transfected with Shh-N (Fig. 6C, left), indicating that a considerable proportion of Shh-N undergoes palmitoylation in the absence of cholesterol modification.

Because a significant fraction of Shh^{C25S} reaches lipid rafts, we then asked if events downstream of lipid raft association are affected. It has been reported that a soluble multimeric protein complex of Shh can be detected in the medium of HEK293T cells expressing Shh, and it has been speculated that the soluble multimeric complex with buried hydrophobic moieties can travel in the morphogenetic field (Zeng et al. 2001). We asked whether formation of soluble multimeric complex is altered in any way by the loss of palmitoylation in Shh^{C25S}. We transfected HEK293T cells with the previous four constructs and isolated the conditioned medium, which was subsequently analyzed by gel filtration chromatography. We then examined the distribution of Shh protein in different fractions from the column (Fig. 7A). As previously reported, a portion of the Shh protein migrated at more than six times its native molecular weight (Zeng et al. 2001). In contrast, all Shh^{C25S} migrated through the column close to predicted molecular weight. Similarly, no immunoreactivity was detected in fractions corresponding to multimeric complex from the conditioned medium collected from cells transfected with Shh-N or Shh-N^{C25S}. To test whether the failure to generate a multimeric complex from Shh^{C25S} is a general phenomenon in diverse cell types, we performed similar experiments by using a variety of cell lines, including CHO, STO, and HeLa cells. Identical results to those from HEK293T were obtained (data not shown). To explore the biochemical properties of Shh multimeric complex and monomer, the fractions corresponding to the multimeric and monomeric Shh, respectively, were subjected to a second round of gel filtration chromatography, and the eluted fractions were analyzed for the presence of Shh by Western blotting (labeled Shh monomer and Shh multimeric complex in Fig. 7A). The elution profiles for Shh multimeric complex and monomer, respectively, were essentially identical to the initial elution profiles, indicating the stability of both forms as well as a lack of interconversion between them under the experimental conditions. Taken together, these results indicate that the lipid modifications, palmitoylation and cholesterylation, are both essential for multimerization of Shh protein.

The activity of Shh multimeric protein complex in inducing Hh responses is significantly greater than that of Shh monomer and Shh-conditioned media

Our studies indicate that *Skn* and *Shh^{C25S}* mutants have reduced Hh signaling, which is likely a consequence of a reduced Hh protein gradient as well as diminished activity of Hh protein in the absence of palmitoylation. Because Shh^{C25S} only generates a monomeric form in cultured cells, it is possible that reduced Shh protein transport is a result of failure to generate a multimeric Shh protein complex. In addition, these results would also

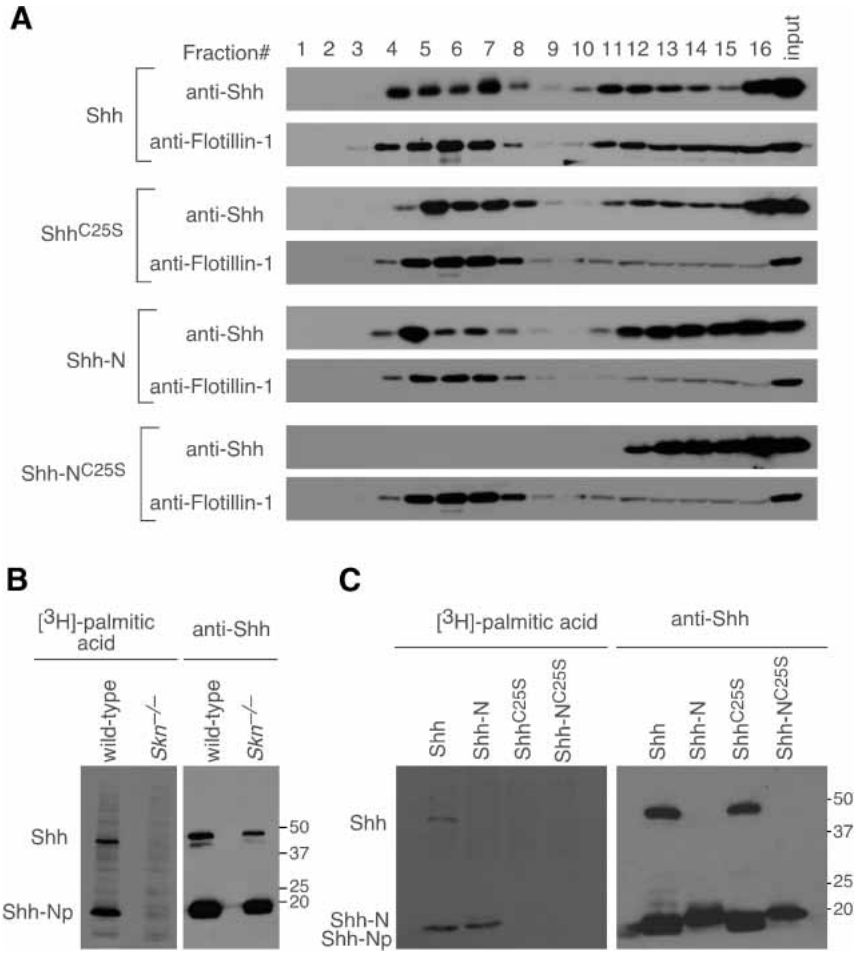

Figure 6. The effects of lipid modification on Hh protein distribution in lipid rafts. (*A*) Western blots of fractions eluted from sucrose gradient probed with anti-Shh and anti-Flotillin-1 (a marker for lipid rafts) antibodies. Lysates from cells transfected with constructs encoding mouse Shh, Shh^{C25S}, Shh-N, and Shh-N^{C25S}, respectively, were processed for sucrose gradient fractionation as described in Materials and Methods. Fractions 4–7 represent lipid raft-containing fractions as indicated by the presence of raft-resident protein Flotillin-1 and caveolin (data not shown). Although Shh, Shh^{C25S}, and Shh-N proteins could be detected in the lipid raft-containing fractions, no Shh-N^{C25S} protein was present in these fractions. (*B*, *left*) Autoradiograph of immunoprecipitates of lysates separated on an SDS-PAGE. Lysates were derived from either wild-type or $Skn^{-/-}$ primary embryonic fibroblasts (MEFs) transfected with an expression construct encoding mouse Shh and grown in [^{3}H]-palmitic acid-containing media. (*Right*) After exposure to film, the same membrane was processed for Western blotting probed with anti-Shh antibodies. Both unprocessed (Shh) and processed (ShhNp) Hh proteins were detected in wild-type and $Skn^{-/-}$ MEFs by Western blotting but only in wild-type MEFs could [^{3}H]-palmitic acid-labeled Hh proteins be detected. (*C*, *left*) Autoradiograph of immunoprecipitates of lysates separated on an SDS-PAGE. Lysates were derived from HEK293 cells transfected with expression constructs encoding mouse Shh, Shh^{C25S}, Shh-N, and Shh-N^{C25S}, respectively, and grown in [^{3}H]-palmitic acid-containing media. (*Right*) Similarly, after exposure to film, the same membrane was processed for Western blotting probed with anti-Shh antibodies. No [^{3}H]-palmitic acid-labeled N-terminal fragment of Shh could be detected in lysates of cells transfected with Shh^{C25S} or Shh-N^{C25S}. Both full-length and processed Shh were labeled by [^{3}H]-palmitic acid, as was Shh-N, indicating that cleavage and cholesterylation of Shh is not an absolute prerequisite for palmitoylation. The proportion of palmitoylated Shh-N remains to be determined. Numbers on the *right* indicate locations of protein size standards.

suggest that Shh multimeric complex may possess higher activity than that of the Shh monomer. To test this hypothesis, gel filtration fractions corresponding to Shh multimeric complex and monomer were pooled and incubated with a Hh reporter cell line, Shh-LIGHT2 (Taipale et al. 2000). Shh multimeric complex induces Hh responses significantly in contrast to Shh monomer, as indicated by the luciferase reporter assay (Fig. 7B, left). When the protein concentration used in the assay is taken into consideration, Shh multimeric complex has ~50-fold higher activity than that of Shh monomer (Fig. 7B, right). The activity of Shh multimeric complex in this assay can be blocked by adding either cyclopamine or Hh-neutralizing antibodies (5E1), indicating that the activity present in the Shh multimeric complex fractions is Hh-dependent. Conditioned media from HEK293T cells transfected with Shh also activated the Hh reporter, and when its activity is normalized to the protein concentration, unfractionated Shh-conditioned media is at least fivefold less active than Shh multimeric complex (Fig. 7B, left; data not shown). These results indicate that Shh multimeric complex is active in inducing Hh responses and is likely the major form involved in this process.

Differential requirement of palmitoylation in Hh multimerization between Drosophila *and vertebrates*

Given the differences in the biological activities of non-palmitoylated Hh^{C85S} and Shh^{C25S} in vivo, we asked whether they also possess different biochemical properties in multimeric complex formation. We expressed various cDNAs encoding Hh, Hh^{C85S}, Hh-N, and Hh-N^{C85S} in *Drosophila* S2 cells by using the GAL4-UAS system (Brand and Perrimon 1993). The conditioned medium was isolated and subjected to analysis by gel filtration chromatography as described above. We then examined the distribution of Hh protein in different fractions from the column (Fig. 7A). Like vertebrate Hh proteins, *Drosophila* Hh protein was also eluted in fractions cor-

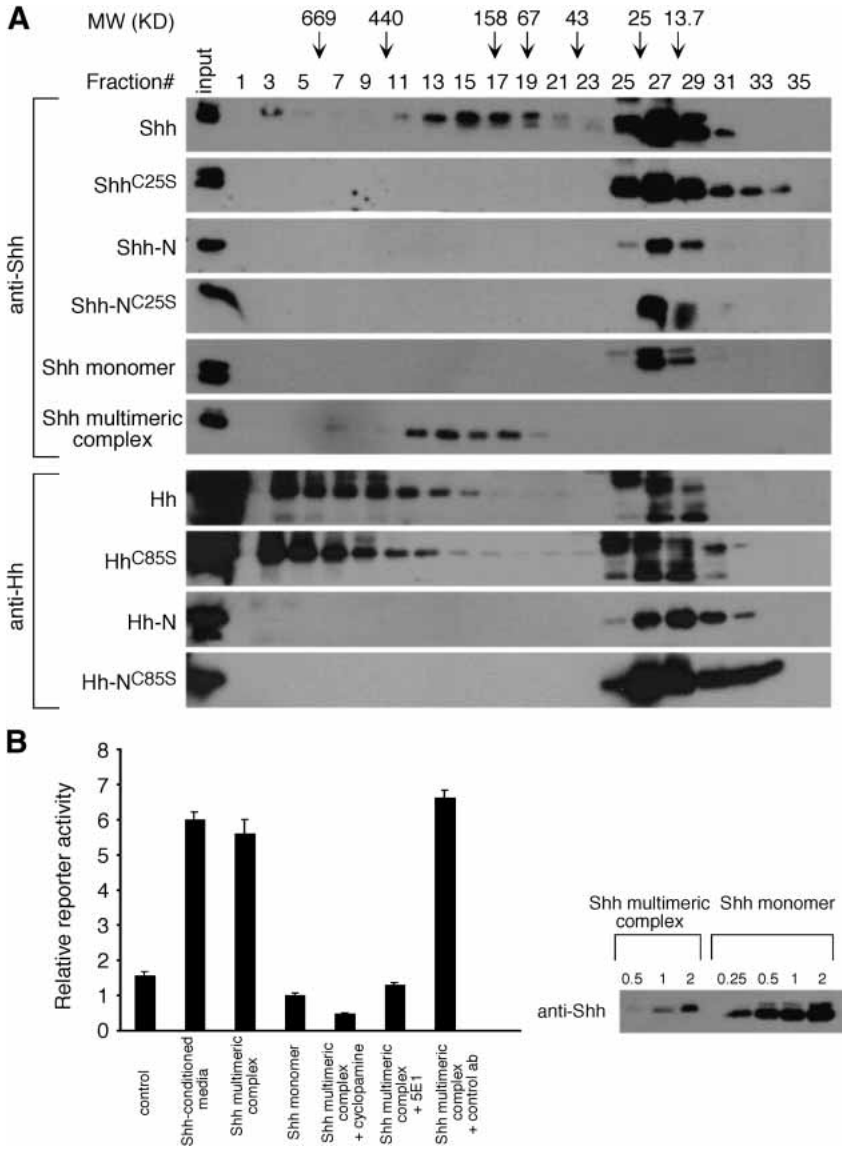

Figure 7. The effects of lipid modification on the generation of a soluble Hedgehog multimeric complex and protein activities. (*A*) Western blots of fractions eluted from gel filtration chromatography probed with anti-Shh antibodies. Supernatants collected from cells transfected with constructs encoding mouse Shh, Shh^{C25S}, Shh-N, and Shh-N^{C25S}, respectively, were processed for gel filtration chromatography as described in Materials and Methods. The fractions in which the molecular weight (MW) standards elute are indicated by arrows. The ratio between Shh multimeric complex and monomer varies between cell lines used in this study. The fractions corresponding to the multimeric and monomeric Shh, respectively, were subjected to a second round of gel filtration chromatography, and the fractions eluted were analyzed for the presence of Shh by Western blotting (labeled Shh monomer and Shh multimeric complex in the figure). Similar experiments were performed by using constructs encoding *Drosophila* Hh, Hh^{C85S}, Hh-N, and Hh-N^{C85S} in S2 cells. Whether the high-MW protein complex that contains *Drosophila* Hh is biologically active or physiologically relevant remains to be determined. (*B*) Activity assays using the Shh-LIGHT2 reporter cell line. Shh multimeric complex exhibits greater activities in inducing Hh-response than Shh monomer as indicated by the luciferase reporter assay. The amount of protein used in this assay is shown on Western blots, in which the number 1 indicates the amount used in this assay, and the other numbers represent fractions or multiplications of that amount. The activity of Shh multimeric complex in this assay can be blocked by adding either cyclopamine or Hh-neutralizing antibodies (5E1) but not by a control antibody. Unfractionated conditioned media from HEK293T cells transfected with Shh also activated the Hh reporter and Shh-conditioned media contains at least fivefold more protein than Shh multimeric complex used in a similar assay.

responding to a higher-molecular-weight protein complex in addition to Hh monomer. The size of the Hh protein complex is greater than that of Shh multimeric complex. Furthermore, similar to vertebrate Shh-N and Shh-N^{C85S}, no immunoreactivity was detected in fractions corresponding to multimeric complex from the conditioned medium collected from cells transfected with *Drosophila* Hh-N or Hh-N^{C85S}. However, in contrast to Shh^{C25S}, which fails to generate a multimer, a multimeric Hh protein complex can still be detected in conditioned medium derived from Hh^{C85S}-transfected S2 cells. Taken together, these results suggest that although both palmitoylation and cholesterylation appear to be essential for vertebrate Hh protein multimerization, palmitoylation is dispensable for *Drosophila* Hh protein complex formation.

Discussion

Our phenotypic analysis of *Skn* and *Shh^{C25S}* mice establishes the essential role of palmitoylation in Hh signaling during vertebrate development. Not only is Shh protein lacking palmitoylation less active than is wild-type Shh protein, the distribution of unpalmitoylated Shh protein in the developing embryos is also disrupted. Insights into the molecular mechanism underlying these observations were engendered by our biochemical studies in cultured cells. We provide the first demonstration that active soluble Shh multimeric complex fails to form in the absence of lipid modifications and that Hh multimeric complex is the major active form in activating Hh responses. These results offer a link between active soluble multimeric complex production and protein gra-

dient generation in the morphogenetic field, uncovering new roles for lipid modification of major signaling molecules (Fig. 8).

The role of lipid modifications in short- and long-range Hedgehog signaling

One of the most puzzling aspects of Hh signaling is the role of lipid modifications in long-range signaling. Reduced long-range Shh signaling activity in patterning the neural tube, limb, and sclerotome in *Skn* and *Shh*^{C25S} mice establishes the essential role of palmitoylation for long-range Hh signaling. Previous studies using a *Shh-N* allele also suggest that cholesterol modification is required for long-range Hh signaling in vertebrates (Lewis et al. 2001). Together, these results highlight the unusual and unexpected function of lipid modification in long-range signaling and point to a novel cellular mechanism for transporting lipid-modified Hh protein. The relative contribution of cholesterol and palmitate to this process is not clear and may vary in different tissues. Previous reports (Pepinsky et al. 1998) suggest that Hh protein is less efficiently palmitoylated in the absence of cho-

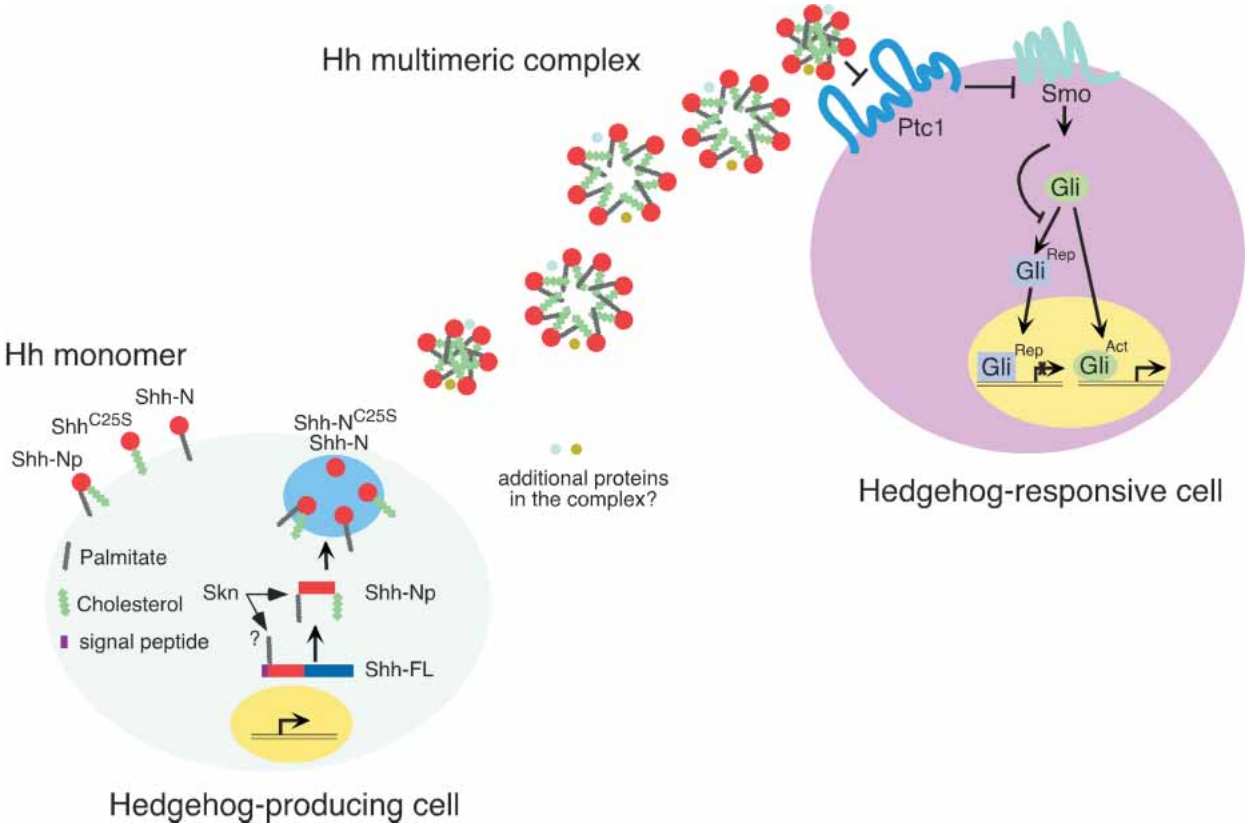

Figure 8. A model of differential Hedgehog protein lipid modification and signaling. A schematic diagram of Hh protein biogenesis and transport. In Hh-producing cells, the Hh precursor molecule (Hh-FL) undergoes autoproteolytic cleavage to generate an N-terminal fragment, the mature form of which (denoted as Hh-Np; p indicates processed) becomes membrane-anchored likely due to the addition of a cholesterol group to the C terminus and a palmitoyl moiety to its N terminus catalyzed by Skn. Proteolytic processing precedes cholesterol modification but may not be a prerequisite for palmitoylation. The destiny of the C-terminal fragment after cleavage is not known. Hh-Np could self-associate spontaneously or in an active process that involves other proteins to generate a multimeric complex (depicted as a mixture of Hh hexamer, heptamer and octamer in this diagram although the actual number of Hh molecules in the multimeric complex may be variable), which is soluble and can be detected in the extracellular environment. Additional proteins may also exist in the Hh multimeric protein complex. The location of Hh multimeric complex formation is not known. The sequence and relationship between proteolytic cleavage, lipid modifications, multimer formation, and trafficking need to be further investigated. Hh multimeric complex is likely the vehicle to be transported to Hh-responsive cells to achieve long-range signaling, although the mechanism by which transport is achieved is unknown. Shh multimeric complex is more active than Shh monomer, and this could potentially be due to differences in affinity for the Hh receptor, Ptc1, or events downstream of ligand binding such as receptor oligomerization or modification. Hh binding to Ptc1 relieves Smo inhibition to allow Smo to transduce the Hh signal. As a result, generation of Gli repressor (Rep) is suppressed, whereas Gli activator (Act) is capable of activating Hh targets in the nucleus. When Shh^{C25S}, Shh-N, and Shh-N^{C25} are expressed in Hh-producing cells under experimental conditions, a significant fraction of Shh-N still undergoes palmitoylation and both Shh-N and Shh^{C25S} reach lipid rafts and can be detected in the extracellular environment in monomeric form. Whether interconversion occurs between Shh multimeric complex and monomer as well as between various Shh monomers in vivo is not known.

lesterylation in vitro. In this case, loss of either type of lipid modification may contribute to the defects in Shh-N mice. Because the limb defects in Shh-N mice are more severe than that in *Skn* or Shh^{C25S} mice, we inferred that cholesterol and palmitate are both required for long-range Hh signaling. However, this conclusion needs to be further tested in vivo using the gene-targeting approach. The neural tube defects in *Shh-N* mice were described, but a detailed analysis was not reported (Lewis et al. 2001). In contrast to the limb phenotype, *Skn* and Shh^{C25S} mutants have severe neural tube defects, at least in the spinal cord, similar to those due to complete loss of *Shh*, raising the question of the relative contributions of cholesterol versus palmitate moieties to long-range Hh signaling in the neural tube. The differences in the severity of limb and neural tube defects in *Skn* and Shh^{C25S} mice could also be due to different tissue sensitivity or distinct requirements for a Hh protein gradient in these two tissues. Moreover, we noticed that Shh^{C25S} neural tube defects are similar to but slightly less severe than those in *Skn* mice, suggesting that Skn may affect either other Hh members or Hh-independent processes. Because both Shh and Ihh signaling are affected in *Skn* mutants, it would be informative to investigate whether Shh-independent phenotypes in the neural tube of *Skn* mice are due to loss of Ihh signaling. Furthermore, because the *Skn* phenotypes are less severe than those in either *Shh* or *Smo* mutants, it remains to be investigated whether this is due to functional redundancy between multiple *Skn* homologs.

The observation that soluble Shh multimeric complex can form is a significant step toward understanding the transport of lipid-modified Hh proteins. An important question is the role of lipid modifications in this process. This issue was addressed by our biochemical studies, which indicate that palmitoylation and cholesterylation are both required for the generation of a Shh multimeric complex in cultured cells. These results also open up the opportunity to further probe the biogenesis of multimeric protein complex in vitro and in vivo. Although the in vivo relevance of Shh multimeric complex needs to be further investigated, it is interesting to speculate that Shh multimeric complex is the major vehicle for Hh transport in the morphogenetic field. Consistent with this idea, Hh protein lacking palmitoylation is confined mainly to its site of synthesis and fails to reach distant Hh-responsive cells in developing embryos. It is also possible Hh multimerization occurs to a different extent in various cell types/tissues in vivo. An important unresolved issue is the location and biochemical mechanism of Shh multimeric complex formation in Hh-producing cells. Our observation that Shh multimeric complex and monomer cannot interconvert spontaneously in vitro suggests that Shh multimeric complex is stable and their formation is likely an active process, possibly requiring a special microenvironment where additional proteins are involved. However, it is also possible that formation of Shh multimeric complex could occur spontaneously in vivo. Soluble Shh monomer may not exist in vivo and was only observed in vitro due to protein overexpression. Shh multimeric complex may be generated within the secretory pathway, or it may form on the plasma membrane or in the extracellular milieu. If Shh multimeric complex plays a key role in mediating Hh protein movement in the morphogenetic field, the mechanism by which Hh multimeric complex is transported is not known. This process may involve an additional protein apparatus or specialized structures (such as cytonemes; Ramirez-Weber and Kornberg 1999).

Given that Shh^{C25S} still possesses residual activity, it is surprising that short-range signaling from the notochord to the floor plate is disrupted in *Skn* and Shh^{C25S} mutants. It is possible that induction of floor plate requires high levels of Hh signal that simply exceed the residual activity of Shh^{C25S}. Alternatively, Hh protein lacking palmitoylation may fail to be transported even short distances to reach adjacent cells.

Palmitoylation and Hh protein multimerization and activity

Largely based on the observation that the majority of purified membrane-tethered N-terminal fragment of Shh protein contains either both types of lipid modification or cholesterol alone, it was inferred that palmitoylation follows cleavage/cholesterylation (Pepinsky et al. 1998). Our labeling experiments provided the first direct demonstration that full-length Shh incorporates [^{3}H] palmitate in cultured cells. In addition, a substantial proportion of Shh-N still undergoes palmitoylation in the absence of cholesterylation. These results raised the issue of the sequence of lipid modifications in vivo as well as the relationship between palmitoylation, cleavage/cholesterylation, and trafficking, which needs to be further investigated.

Our demonstration that the soluble vertebrate Shh multimeric complex exhibits significantly greater activity than do Shh monomer and Shh-conditioned media in inducing Hh responses strongly suggests that the Hh multimeric complex is the major active form produced by Hh-secreting cells. Consistent with this observation, lack of Shh protein lipid modification leads to disruption of Hh multimerization and reduced activity in vitro and in vivo. It thus appears that Hh multimerization is not only involved in transport but also required for its activity. Because Shh protein lacking both palmitoylation and cholesterylation appears to be less active than that without palmitoylation in vitro (Y.-J. Li and P.-T. Chuang, unpubl.) and in vivo, we concluded that Shh monomer without any lipid modification is less active than that with one type of lipid modification. The biochemical basis underlying the differential activities between Shh multimeric complex and various forms of monomer is not known and possibly reflects their distinct biochemical interactions with the Hh receptor Ptc1 (or Ptc2) or Hh-binding protein Hip1. Previous studies indicated that purified Shh-Np and Shh-N exhibit similar affinity for binding to Ptc1 (Pepinsky et al. 1998). However, the major constituent of Shh-Np was not known in this assay,

and it is possible that multimeric Hh complex actually either has higher intrinsic affinity for Ptc1 or is capable of eliciting greater biological responses, for instance, through receptor oligomerization or binding to coreceptor proteins. It is also not clear how stable the Hh lipid modifications are in vivo. If conversion occurs between Hh multimeric complex and monomers, as well as between various monomers in vivo, they may provide a means to regulate the activities of Hh signaling by controling the amounts of Hh multimeric complex and monomer(s) present in the morphogenetic field in various tissues.

Hh protein multimerization and activity in fly and vertebrate

Because many aspects of Hh signaling are highly conserved from fly to mammals (Ingham and McMahon 2001), it is unanticipated that the roles of lipid modifications in *Drosophila* versus vertebrate Hh signaling do not seem to be identical. Not only is the requirement for lipid modifications for Hh activity different in these two systems, their contributions to Hh protein distribution are also different. Our biochemical studies on *Drosophila* Hh protein identified a high-molecular-weight Hh protein complex with size that appears to be significantly greater than that in vertebrates. It is possible that the *Drosophila* Hh complex has a different biochemical composition from that of the vertebrate Shh multimeric complex. Alternatively, this complex may not represent a physiologically relevant form for Hh signaling in vivo. In this case, the mechanism for transporting lipid-modified Hh proteins in fly and vertebrate systems could be fundamentally different. Interestingly, *Drosophila* Hh protein lacking palmitoylation maintains its ability to generate a high-molecular-weight complex. This is consistent with the observation that Hh protein lacking palmitoylation is readily secreted into the conditioned media of S2 cells subjected to RNAi-mediated *ski* knockdown (Chamoun et al. 2001). It is not clear whether these discrepancies between vertebrate and *Drosophila* Hh protein are due to intrinsic differences in their biochemical properties or due to the microenvironment in which the Hh protein is generated and processed. Understanding the biochemical basis of these differences will shed new light on the molecular mechanisms as well as the evolution of Hh signaling in diverse organisms.

A general role of palmitoylation in major signaling pathways?

Palmitoylation is one of the most frequent posttranslational modifications found on proteins. In most cases, palmitoylation occurs on membrane proteins and affects their intracellular localization and function (Linder and Deschenes 2003). In addition to potential roles in membrane trafficking, it is unexpected that Hh palmitoylation plays a key role in Hh protein transport and signaling activity, suggesting potential roles of palmitoylation in a wide range of secreted signaling molecules. Consistent with this notion, palmitoylation of Wnt protein was shown to be required for its activity (Willert et al. 2003). Given the similarity between the basic design of Hh and Wnt pathways (Kalderon 2002; Nusse 2003), it is tempting to speculate that lipid modification might play additional roles in Wnt signaling, similar to those uncovered in Hh signaling. Furthermore, if lipid modification was adopted by signaling pathways to confer novel functions, it may not be surprising to identify essential roles played by palmitoylation in other major signal transduction cascades. Lessons learned from studying Hh signaling will lay important foundations for these investigations.

Materials and methods

Standard molecular biology techniques were performed as described (Sambrook and Russell 2001).

Generation of transgenic mice

cDNAs encoding Shh, Shh^{C25S}, and Shh-N^{C25S} were cloned into a transgenic vector in which the cDNAs are placed under the regulation of the *Prx1*-derived regulatory element (Logan et al. 2002). The purified inserts of the transgenic constructs were injected into the pronuclei of fertilized eggs following standard procedures (Nagy et al. 2003). Embryos were collected at 18.5 dpc, and skeletal preparation was performed as described (Nagy et al. 2003).

Generation of Skn knockout and Shh^{C25S} mice

There are at least two *Skn*-like genes in mouse. One (BC008159) is more closely related to *Drosophila ski* and was used in this study. The other homolog (AK003605) may represent a more distant member of the family, and its function is not known. To construct a positive/negative targeting vector for removing exon 2 of the *Skn* gene (the resulting allele is designated *SknΔE2*), a 3.5-kb genomic fragment containing exon 2 of *Skn* and sequences upstream of exon 2 was amplified by PCR and used as the 5′ region of homology (Supplementary Fig. 1). A *loxP* site was inserted in the 5′ region of homology, ~70 bp upstream of exon 2. A 3.5-kb fragment containing sequences downstream of exon 2 was used as the 3′ region of homology and was inserted upstream of the MC1-*tk*-pA cassette. The genomic fragments were sequenced to verify their identities. A PGK-*neo*-pA cassette, which also carries a *loxP* site at its 3′ end, was inserted between the 5′ and 3′ homology regions. Upon Cre-mediated excision of sequences between the two *loxP* sites (including the PGK-*neo*-pA cassette), exon 2 will be removed and *SknΔE2* will be generated. A similarly strategy was used to remove exon 9 of *Skn* (the resulting allele is designated *SknΔE9*; Supplementary Fig. 2). To generate a *Shh^{C25S}* allele, a single base pair change (G to C) was introduced in the 2.6-kb genomic fragment used as the 5′ region of homology, resulting in a Cys-to-Ser change at amino acid position 25 of Shh protein (Supplementary Fig. 3). The 5′ region of homology encompasses exon 1 of *Shh* and sequences upstream of exon 1. A 3.3-kb fragment containing sequences downstream of exon 1 was used as the 3′ region of homology and was inserted upstream of the MC1-*tk*-pA cassette. A PGK-*neo*-pA cassette, flanked by *FRT* sites, was inserted between the 5′ and 3′ homology regions.

E14Tg2A.4 (E14) feeder-independent embryonic stem (ES) cells (Nichols et al. 1990) were electroporated with a SalI-lin-

earized targeting vectors and selected in G418 and FIAU as described (Joyner 2000). Heterozygous E14 ES cells were injected into blastocysts of C57BL/6 strain mice to generate germline chimeras. Chimeric males were mated with C57BL/6, 129/Sv, 129/Ola, or Swiss-Webster females (to maintain the *Skn* and Shh^{C25S} alleles in different genetic backgrounds), and heterozygous animals were identified by Southern blotting of tail-tip DNA. Germline transmission was obtained from multiple independently targeted ES cell clones for all three targeting vectors. Heterozygous *Skn* animals were crossed to animals expressing β-*actin*::*Cre* (Lewandoski et al. 1997) to remove sequences between the two *loxP* sites (including the PGK-*neo*-PA cassette). Heterozygous Shh^{C25S} animals were mated with *FLPe* animals (Dymecki 1996) to remove the PGK-*neo*-pA selection cassette.

Histology, in situ hybridization, and immunohistochemistry

Histological analysis, whole-mount in situ hybridization using digoxigenin-labeled probes, and section in situ hybridization using ^{33}P-labeled riboprobes were performed as described (Wilkinson and Nieto 1993). Immunohistochemistry using anti-Shh antibodies was performed as described (Gritli-Linde et al. 2001; Kawakami et al. 2002).

Membrane fractionation and lipid raft isolation

cDNAs encoding Shh, Shh^{C25S}, Shh-N, and Shh-N^{C25S} were cloned into the mammalian expression vector pcDNA3 (Invitrogen). The resulting constructs were transfected into HEK293 cells by using Lipofectamine reagent (Invitrogen). Lipid rafts were isolated as follows (Taipale et al. 2000): cells from a 60-mm dish were lysed and collected in 1.5 mL of lysis solution (10 mM NaHPO4 at pH 6.5, 150 mM NaCl, 0.5 mM PMSF, 1% Triton X-100, 2 µg/mL Pepstatin A, 10 µg/mL leupeptin, 5 µg/mL aprotinin) at 4°C. The cell lysate were then mixed with same volume of 80% sucrose. Eight sucrose density steps (35.625–5%, 4.375%/step, 1 mL/step; made in above solution, without detergent) were layered onto the 40% sucrose lysate, and centrifugation proceeded for 20 h. Sixteen fractions (0.6875 mL/fraction) were collected. The same volume of each fraction was separated with 12% SDS-PAGE and transferred onto PVDF membrane for Western blotting. The membranes were probed with rabbit polyclonal antibodies against Shh and antibodies against lipid raft resident proteins Flotillin-1 and caveolin-1 (BD Biosciences).

Gel filtration chromatography

For studies on vertebrate Hh proteins, expression constructs encoding Shh, Shh^{C25S}, Shh-N, and Shh-N^{C25S} were transfected into several established cell lines (including HEK293T, CHO, STO, and HeLa) using Lipofectamine reagent (Invitrogen). Serum-free conditioned media (Optimem, supplemented with Insulin-Transferrin-Selenium-A, Invitrogen) from cultured cells transfected with different forms of Shh were collected and filtered through a 0.2-µm filter and then ultracentrifuged at 100,000*g* for 2 h. The supernatants were concentrated by using a Centriprep YM-10 (Amicon) and loaded on to a Superdex 200 (Amersham Biotech) gel filtration column that had been equilibrated with PBS/0.001% NP-40. Every two fractions eluted were precipitated with TCA or immunoprecipitated with mouse anti-Shh antibody (5E1; Developmental Studies Hybridoma Bank), resolved by 12% SDS-PAGE, and immunoblotted with rabbit polyclonal antibodies against Shh.

For a second round of gel filtration chromatography on pooled fractions, fraction no. 10–18, which contains the Shh multimeric complex, and fraction no. 25–31, which contains the Shh monomers, were combined respectively; stored at 4°C for 12–20 h; and then concentrated with a Centriprep YM-10. The concentrated samples were loaded onto the Superdex 200 gel filtration column. Separation, collection, and detection were performed as described above.

For studies on *Drosophila* Hh proteins, insect S2 cells were grown in Schneider's *Drosophila* medium (Invitrogen) supplemented with 10% fetal bovine serum (Invitrogen), L-glutamine, and penicillin/streptomycin. The S2 cells were cotransfected with the expression construct encoding actin-Gal4 and various UAS plasmids, including UAS-hh, UAS-hh^{C85S}, UAS-hh-N, and UAS-hh-N^{C85S} with Effectene (QIAGEN). Twelve to eighteen hours after transfection, the S2 media were switched to SF-900 II serum-free medium (Invitrogen). Two days later, the conditioned media were harvested and processed in the same way as described above for vertebrate Hh proteins.

Isotope labeling with [^{3}H]-palmitic acid

HEK293 cells and primary mouse embryonic fibroblasts (MEFs) derived from wild-type or $Skn^{-/-}$ mouse embryos at 10.5 dpc were transfected with Lipofectamine reagent (Invitrogen). Thirty-six hours after transfection, the cells were incubated for 4 h in 10% dialyzed FBS in DMEM containing 500 µCi/mL [9,10-^{3}H] palmitate (Perkin Elmer). The cells were washed with PBS, then harvested by scraping in lysis buffer containing 50 mM Tris (pH 7.5), 150 mM NaCl, 2 mM EDTA, 1% Triton X-100, 0.5% sodium deoxycholate, 0.5 mM DTT, 1 mM PMSF, and 2 µg/mL each of aprotinin, leupeptin, and pepstatin A. Insoluble materials were sedimented by centrifugation at 20,000*g* for 30 min at 4°C. The supernatant were mixed with mouse anti-Shh antibody (5E1) and protein G beads overnight; the beads were washed, separated by SDS-PAGE, and transferred onto a PVDF membrane. The membrane was sprayed with Enhance solution (Perkin Elmer) and exposed to films for 7–14 d. The same PVDF membrane was then probed with rabbit polyclonal antibodies against Shh.

Hedgehog activity assay

Shh-LIGHT2 cells were cultured to confluency in 24-well plates using DMEM media containing 10% (v/v) bovine calf serum, 150 µg/mL zeocin, and 400 µg/mL G418. For activity assays, Shh-LIGHT2 cells were switched to DMEM containing 0.5% bovine calf serum and incubated with (1) various dilutions of conditioned media collected from HEK293T cells transfected with Shh, Shh^{C25S}, Shh-N, or Shh-N^{C25S} expression constructs and (2) various dilutions of fractions from gel filtration chromatography. To test the specificity of Hh activities in the conditioned media or gel filtration fractions, cyclopamine (Poisonous Plant Research Laboratory, ARS-USDA) or anti-Shh monoclonal antibodies (5E1) were also added to the media to reach a final concentration of 4 µM and 1 µg/mL, respectively. After incubation for 2 d at 37°C, cellular firefly luciferase and Renilla luciferase activities were measured by using chemiluminescence. To estimate the relative Hh protein concentrations in the conditioned media and fractions from gel filtration chromatography, the media or fractions at different dilutions were separated on 12% SDS-PAGE, probed with rabbit polyclonal anti-Shh antibody, and detected by using the ECL kit (Amersham Biotech).

Immunostaining

CHO cells grown on chamber slides were transfected with an expression construct encoding MYC-tagged Skn or cotrans-

fected with constructs encoding MYC-tagged Skn and Shh with Lipofectamine reagent (Invitrogen). Thirty-six to forty-eight hours after transfection the cells were fixed with 4% paraformaldehyde in PBS for 10 min, washed with PBS, permeabilized in 0.2% Triton in PBS for 15 min, blocked with 2.5% goat serum and 0.02% Triton in PBS for 1 h, and incubated with 1:400 dilution of primary antibodies in blocking buffer overnight at 4°C. The primary antibodies used include mouse anti-MYC antibodies (9E10, Santa Cruz Biotech), mouse anti-KDEL antibodies (StressGen Biotechnologies), rabbit polyclonal anti-Shh antibodies, rabbit anti-Myc antibodies (Cell Signaling Biotech), and mouse anti-Shh antibody (5E1). The cells were then washed extensively with 0.02% Triton in PBS, incubated with goat anti-rabbit Alexa 488 and goat anti-mouse Alexa 594 antibodies (1: 400 dilution) in blocking buffer for 1 h at room temperature, washed extensively, and mounted onto slides for fluorescence microscopy.

Acknowledgments

We thank Dr. Andy McMahon (Harvard University) for providing *Ihh* mutant mice, James Martin for the *Prx1* expression construct, Tom Kornberg for supplying *Drosophila* hedgehog expression vectors and antibodies, Phil Beachy for Shh-LIGHT2 cells, and those who supplied probes. We thank T'Nay Kawcak for help with targeting vector construction; Yongmei Hu for help with ES cell work; and Stephanie Paula, Franchesca Liao, Julie Qiao, Rachel Sutherland, and Haixia Huang for assistance with sectioning, in situ hybridization, and immunohistochemistry. We thank members of the Chuang laboratory for helpful discussion and Chris Wilson, Tony Gerber, Didier Stainier, and Matthias Hebrok for critical reading of the manuscript. Work in the Chuang laboratory was supported by an National Institutes of Health grant (HL67822).

The publication costs of this article were defrayed in part by payment of page charges. This article must therefore be hereby marked "advertisement" in accordance with 18 USC section 1734 solely to indicate this fact.

References

Amanai, K. and Jiang, J. 2001. Distinct roles of Central missing and Dispatched in sending the Hedgehog signal. *Development* **128:** 5119–5127.

Ang, S.L., Wierda, A., Wong, D., Stevens, K.A., Cascio, S., Rossant, J., and Zaret, K.S. 1993. The formation and maintenance of the definitive endoderm lineage in the mouse: Involvement of HNF3/forkhead proteins. *Development* **119:** 1301–1315.

Bellaiche, Y., The, I., and Perrimon, N. 1998. Tout-velu is a *Drosophila* homologue of the putative tumour suppressor EXT-1 and is needed for Hh diffusion. *Nature* **394:** 85–88.

Brand, A.H. and Perrimon, N. 1993. Targeted gene expression as a means of altering cell fates and generating dominant phenotypes. *Development* **118:** 401–415.

Briscoe, J. and Ericson, J. 1999. The specification of neuronal identity by graded Sonic Hedgehog signalling. *Semin. Cell. Dev. Biol.* **10:** 353–362.

———. 2001. Specification of neuronal fates in the ventral neural tube. *Curr. Opin. Neurobiol.* **11:** 43–49.

Burke, R., Nellen, D., Bellotto, M., Hafen, E., Senti, K.A., Dickson, B.J., and Basler, K. 1999. Dispatched, a novel sterol-sensing domain protein dedicated to the release of cholesterol-modified hedgehog from signaling cells. *Cell* **99:** 803–815.

Chamoun, Z., Mann, R.K., Nellen, D., von Kessler, D.P., Bellotto, M., Beachy, P.A., and Basler, K. 2001. Skinny hedgehog, an acyltransferase required for palmitoylation and activity of the hedgehog signal. *Science* **293:** 2080–2084.

Chiang, C., Litingtung, Y., Lee, E., Young, K.E., Corden, J.L., Westphal, H., and Beachy, P.A. 1996. Cyclopia and defective axial patterning in mice lacking Sonic hedgehog gene function. *Nature* **383:** 407–413.

Chuang, P.-T. and McMahon, A.P. 1999. Vertebrate Hedgehog signalling modulated by induction of a Hedgehog-binding protein. *Nature* **397:** 617–621.

Deutsch, U., Dressler, G.R., and Gruss, P. 1988. Pax 1, a member of a paired box homologous murine gene family, is expressed in segmented structures during development. *Cell* **53:** 617–625.

Dymecki, S.M. 1996. Flp recombinase promotes site-specific DNA recombination in embryonic stem cells and transgenic mice. *Proc. Natl. Acad. Sci.* **93:** 6191–6196.

Echelard, Y., Epstein, D.J., St-Jacques, B., Shen, L., Mohler, J., McMahon, J.A., and McMahon, A.P. 1993. Sonic hedgehog, a member of a family of putative signaling molecules, is implicated in the regulation of CNS polarity. *Cell* **75:** 1417–1430.

Fan, C.M. and Tessier-Lavigne, M. 1994. Patterning of mammalian somites by surface ectoderm and notochord: Evidence for sclerotome induction by a hedgehog homolog. *Cell* **79:** 1175–1186.

Fan, C.M., Porter, J.A., Chiang, C., Chang, D.T., Beachy, P.A., and Tessier, L.M. 1995. Long-range sclerotome induction by sonic hedgehog: Direct role of the amino-terminal cleavage product and modulation by the cyclic AMP signaling pathway. *Cell* **81:** 457–465.

Goodrich, L.V., Johnson, R.L., Milenkovic, L., McMahon, J.A., and Scott, M.P. 1996. Conservation of the hedgehog/patched signaling pathway from flies to mice: Induction of a mouse patched gene by Hedgehog. *Genes & Dev.* **10:** 301–312.

Gritli-Linde, A., Lewis, P., McMahon, A.P., and Linde, A. 2001. The whereabouts of a morphogen: Direct evidence for short- and graded long-range activity of hedgehog signaling peptides. *Dev. Biol.* **236:** 364–386.

Han, C., Belenkaya, T.Y., Wang, B., and Lin, X. 2004. *Drosophila* glypicans control the cell-to-cell movement of Hedgehog by a dynamin-independent process. *Development* **131:** 601–611.

Ho, K.S. and Scott, M.P. 2002. Sonic hedgehog in the nervous system: Functions, modifications and mechanisms. *Curr. Opin. Neurobiol.* **12:** 57–63.

Hofmann, K. 2000. A superfamily of membrane-bound O-acyltransferases with implications for wnt signaling. *Trends Biochem. Sci.* **25:** 111–112.

Ingham, P.W. and McMahon, A.P. 2001. Hedgehog signaling in animal development: Paradigms and principles. *Genes & Dev.* **15:** 3059–3087.

Jones, C.M., Lyons, K.M., and Hogan, B.L. 1991. Involvement of Bone Morphogenetic Protein-4 (BMP-4) and Vgr-1 in morphogenesis and neurogenesis in the mouse. *Development* **111:** 531–542.

Joyner, A.L. 2000. *Gene targeting: A practical approach*, 2nd ed. Oxford University Press, Oxford.

Kalderon, D. 2002. Similarities between the Hedgehog and Wnt signaling pathways. *Trends Cell. Biol.* **12:** 523–531.

Kawakami, T., Kawcak, T., Li, Y.-J., Zhang, W., Hu, Y., and Chuang, P.-T. 2002. Mouse dispatched mutants fail to distribute hedgehog proteins and are defective in hedgehog sig-

naling. *Development* **129:** 5753–5765.
Kohtz, J.D., Lee, H.Y., Gaiano, N., Segal, J., Ng, E., Larson, T., Baker, D.P., Garber, E.A., Williams, K.P., and Fishell, G. 2001. N-terminal fatty-acylation of sonic hedgehog enhances the induction of rodent ventral forebrain neurons. *Development* **128:** 2351–2363.
Kraus, P., Fraidenraich, D., and Loomis, C.A. 2001. Some distal limb structures develop in mice lacking Sonic hedgehog signaling. *Mech. Dev.* **100:** 45–58.
Le Douarin, N.M. and Halpern, M.E. 2000. Discussion point. Origin and specification of the neural tube floor plate: Insights from the chick and zebrafish. *Curr. Opin. Neurobiol* **10:** 23–30.
Lee, J.D. and Treisman, J.E. 2001. Sightless has homology to transmembrane acyltransferases and is required to generate active Hedgehog protein. *Curr. Biol.* **11:** 1147–1152.
Lee, J.D., Kraus, P., Gaiano, N., Nery, S., Kohtz, J., Fishell, G., Loomis, C.A., and Treisman, J.E. 2001. An acylatable residue of Hedgehog is differentially required in *Drosophila* and mouse limb development. *Dev. Biol.* **233:** 122–136.
Lewandoski, M., Meyers, E.N., and Martin, G.R. 1997. Analysis of Fgf8 gene function in vertebrate development. *Cold Spring Harb. Symp. Quant. Biol.* **62:** 159–168.
Lewis, P.M., Dunn, M.P., McMahon, J.A., Logan, M., Martin, J.F., St-Jacques, B., and McMahon, A.P. 2001. Cholesterol modification of sonic hedgehog is required for long-range signaling activity and effective modulation of signaling by Ptc1. *Cell* **105:** 599–612.
Linder, M.E. and Deschenes, R.J. 2003. New insights into the mechanisms of protein palmitoylation. *Biochemistry* **42:** 4311–4320.
Litingtung, Y. and Chiang, C. 2000. Specification of ventral neuron types is mediated by an antagonistic interaction between Shh and Gli3. *Nat. Neurosci.* **3:** 979–985.
Litingtung, Y., Dahn, R.D., Li, Y., Fallon, J.F., and Chiang, C. 2002. Shh and Gli3 are dispensable for limb skeleton formation but regulate digit number and identity. *Nature* **418:** 979–983.
Logan, M., Martin, J.F., Nagy, A., Lobe, C., Olson, E.N., and Tabin, C.J. 2002. Expression of Cre recombinase in the developing mouse limb bud driven by a Prxl enhancer. *Genesis* **33:** 77–80.
Marti, E., Bumcrot, D.A., Takada, R., and McMahon, A.P. 1995. Requirement of 19K form of Sonic hedgehog for induction of distinct ventral cell types in CNS explants. *Nature* **375:** 322–325.
McMahon, A.P., Ingham, P.W., and Tabin, C.J. 2003. Developmental roles and clinical significance of hedgehog signaling. *Curr. Top. Dev. Biol.* **53:** 1–114.
Micchelli, C.A., The, I., Selva, E., Mogila, V., and Perrimon, N. 2002. Rasp, a putative transmembrane acyltransferase, is required for Hedgehog signaling. *Development* **129:** 843–851.
Nagy, A., Gertsenstein, M., Vintersten, K., and Behringer, R. 2003. *Manipulating the mouse embryo: A laboratory manual*, 3rd ed. Cold Spring Harbor Laboratory Press, Cold Spring Harbor, NY.
Nichols, J., Evans, E.P., and Smith, A.G. 1990. Establishment of germ-line-competent embryonic stem (ES) cells using differentiation inhibiting activity. *Development* **110:** 1341–1348.
Niswander, L. and Martin, G.R. 1992. Fgf-4 expression during gastrulation, myogenesis, limb and tooth development in the mouse. *Development* **114:** 755–768.
Nusse, R. 2003. Wnts and Hedgehogs: Lipid-modified proteins and similarities in signaling mechanisms at the cell surface. *Development* **130:** 5297–5305.
Pepinsky, R.B., Zeng, C., Wen, D., Rayhorn, P., Baker, D.P., Williams, K.P., Bixler, S.A., Ambrose, C.M., Garber, E.A., Miatkowski, K., et al. 1998. Identification of a palmitic acid-modified form of human Sonic hedgehog. *J. Biol. Chem.* **273:** 14037–14045.
Pierani, A., Brenner-Morton, S., Chiang, C., and Jessell, T.M. 1999. A sonic hedgehog-independent, retinoid-activated pathway of neurogenesis in the ventral spinal cord. *Cell* **97:** 903–915.
Placzek, M., Dodd, J., and Jessell, T.M. 2000. Discussion point: The case for floor plate induction by the notochord. *Curr. Opin. Neurobiol.* **10:** 15–22.
Porter, J.A., Young, K.E., and Beachy, P.A. 1996. Cholesterol modification of hedgehog signaling proteins in animal development. *Science* **274:** 255–259.
Ramirez-Weber, F.-A. and Kornberg, T.B. 1999. Cytonemes: Cellular processes that project to the principal signaling center in *Drosophila* imaginal discs. *Cell* **97:** 599–607.
Riddle, R.D., Johnson, R.L., Laufer, E., and Tabin, C. 1993. Sonic hedgehog mediates the polarizing activity of the ZPA. *Cell* **75:** 1401–1416.
Rietveld, A., Neutz, S., Simons, K., and Eaton, S. 1999. Association of sterol- and glycosylphosphatidylinositol-linked proteins with *Drosophila* raft lipid microdomains. *J. Biol. Chem.* **274:** 12049–12054.
Roelink, H., Porter, J.A., Chiang, C., Tanabe, Y., Chang, D.T., Beachy, P.A., and Jessell, T.M. 1995. Floor plate and motor neuron induction by different concentrations of the amino-terminal cleavage product of sonic hedgehog autoproteolysis. *Cell* **81:** 445–455.
Sambrook, J. and Russell, D.W. 2001. *Molecular cloning: A laboratory manual*. Cold Spring Harbor Laboratory Press, Cold Spring Harbor, NY.
Sasaki, H. and Hogan, B.L. 1993. Differential expression of multiple fork head related genes during gastrulation and axial pattern formation in the mouse embryo. *Development* **118:** 47–59.
St-Jacques, B., Hammerschmidt, M., and McMahon, A.P. 1999. Indian hedgehog signaling regulates proliferation and differentiation of chondrocytes and is essential for bone formation. *Genes & Dev.* **13:** 2072–2086.
Suzuki, H.R., Sakamoto, H., Yoshida, T., Sugimura, T., Terada, M., and Solursh, M. 1992. Localization of HstI transcripts to the apical ectodermal ridge in the mouse embryo. *Dev. Biol.* **150:** 219–222.
Taipale, J., Chen, J.K., Cooper, M.K., Wang, B., Mann, R.K., Milenkovic, L., Scott, M.P., and Beachy, P.A. 2000. Effects of oncogenic mutations in Smoothened and Patched can be reversed by cyclopamine. *Nature* **406:** 1005–1009.
Tajbakhsh, S., Rocancourt, D., Cossu, G., and Buckingham, M. 1997. Redefining the genetic hierarchies controlling skeletal myogenesis: Pax-3 and Myf-5 act upstream of MyoD. *Cell* **89:** 127–138.
Takei, Y., Ozawa, Y., Sato, M., Watanabe, A., and Tabata, T. 2004. Three *Drosophila* EXT genes shape morphogen gradients through synthesis of heparan sulfate proteoglycans. *Development* **131:** 73–82.
te Welscher, P., Zuniga, A., Kuijper, S., Drenth, T., Goedemans, H.J., Meijlink, F., and Zeller, R. 2002. Progression of vertebrate limb development through SHH-mediated counteraction of GLI3. *Science* **298:** 827–830.
The, I., Bellaiche, Y., and Perrimon, N. 1999. Hedgehog movement is regulated through tout velu-dependent synthesis of a heparan sulfate proteoglycan. *Mol. Cell* **4:** 633–639.
Wijgerde, M., McMahon, J.A., Rule, M., and McMahon, A.P. 2002. A direct requirement for Hedgehog signaling for normal specification of all ventral progenitor domains in the

presumptive mammalian spinal cord. *Genes & Dev.* **16:** 2849–2864.

Wilkinson, D.G. and Nieto, M.A. 1993. Detection of messenger RNA by in situ hybridization to tissue sections and whole mounts. *Methods Enzymol.* **225:** 361–373.

Willert, K., Brown, J.D., Danenberg, E., Duncan, A.W., Weissman, I.L., Reya, T., Yates III, J.R., and Nusse, R. 2003. Wnt proteins are lipid-modified and can act as stem cell growth factors. *Nature* **423:** 448–452.

Yang, Y., Drossopoulou, G., Chuang, P.-T., Duprez, D., Marti, E., Bumcrot, D., Vargesson, N., Clarke, J., Niswander, L., McMahon, A., et al. 1997. Relationship between dose, distance and time in Sonic Hedgehog-mediated regulation of anteroposterior polarity in the chick limb. *Development* **124:** 4393–4404.

Zeng, X., Goetz, J.A., Suber, L.M., Scott Jr., W.J., Schreiner, C.M., and Robbins, D.J. 2001. A freely diffusible form of Sonic hedgehog mediates long-range signalling. *Nature* **411:** 716–720.